EVOLUTIONARY PATTERNS OF LATE QUATERNARY BIRDS FROM THE LA BREA TAR PITS DURING THE LAST GLACIAL-INTERGLACIAL CYCLE

A Thesis

Presented to the

Faculty of

California State Polytechnic University, Pomona

In Partial Fulfillment

Of the Requirements for the Degree

Master of Science

In

Geological Sciences

By

Katherine L. Long

2018

SIGNATURE PAGE

THESIS	EVOLUTIONARY PATTERNS OF LATE QUATERNARY BIRDS FROM THE LA BREA TAR PITS DURING THE LAST GLACIAL-INTERGLACIAL CYCLE
AUTHOR	Katherine L. Long
DATE SUBMITTED	Spring 2018
	Geological Sciences Department

Dr. Bryan P. Murray ______________________________
Thesis Committee Chair
Geological Sciences

Dr. Jeffrey S. Marshall ______________________________
Geological Sciences

Dr. Donald Prothero ______________________________
Geological Sciences

ACKNOWLEDGEMENTS

This thesis project could not have been done without the aid and guidance of several individuals. First, I’d like to thank Dr. Kenneth E. Campbell for access to the avian collections at Rancho La Brea, as well as its collections managers, Aisling Farrell and Gary Takeuchi.

I thank Carla Cicero and Rauri Bowie of the University of California Museum of Vertebrate Zoology in Berkeley for their help with access to their modern bird collections.

Lastly, I’d like to most of all thank my graduate advisor Dr. Don Prothero. Don has gone above and beyond with his work in vertebrate paleontology and to his students. Thank you Don for pushing me seemingly endlessly to get this and other projects done.

ABSTRACT

The concept of selective adaptation is classically illustrated by Darwin's Galapagos finches, which exemplify a population response to environmental change. Galapagos finches are famous for showing rapid changes in phenotype (especially body size and bill morphology) in response to changes in habitats, such as vegetation and climate transitions. This model is often cited as the norm for how species, and especially birds, should respond to a changing environment. My study investigates a sample of four distinct avian species at Rancho La Brea persisting through record of specimens from La Brea tar pits, ranging from 35,000 years ago through the last complete glacial-interglacial cycle to the early Holocene. Complete stasis in size and limb robustness has been proven in nearly every La Brea species, including previously studied (and mostly larger) avifauna. Stasis, in which species retain a stable morphology over extended periods of time, is found in every bird species at La Brea, even during the coldest periods of climate about 20,000 years ago, when snowy forests replaced the modern chaparral. I examined the only common smaller birds at La Brea: the Pleistocene relative of the Black Vulture (*Coragyps occidentalis*), Magpie (*Pica nutalli*), Raven (*Corvus corax*), and Meadowlark (*Sturnella neglecta*). Although the sample size is limited, none of these smaller birds show any response to environmental changes but are completely static through the interval. This demonstrates that even small species of birds are less responsive to climate change that the prevailing model suggests.

TABLE OF CONTENTS

LIST OF TABLES

LIST OF FIGURES

CHAPTER 1 - INTRODUCTION

It has been long taught in evolutionary biology that species are very sensitive and responsive to environmental stressors. Many avian species have been examined in this regard. In a study examining 24 Australian passerine species, 67% showed significant morphological changes from 1960-2007 that correlated with changes in temperature in their native regions (Gardner 2014). A notable example of environmental adaption is Darwin’s Galapagos Finches (Weiner, 1995; Grant and Weiner, 1999; Grant and Grant, 2007). In fact, the documentation of the finches convincingly demonstrates extremely rapid adaptive evolution (Gardner 2014). After a drought in 1977, observers documented a drastic episode of natural selection that resulted in a massive shift in sex ratios in one species of finch. This was due to selection on body and beak size (due to seed availability), in which males are larger. At the start of the drought there were approximately 600 males and 600 females, and by the end there were roughly 150 males and a decimated female population (Weiner,1995). Because of these observable circumstances in the finch population, it’s no wonder their detailed recounts are cited most often when discussing rudimentary laws of evolution and its mechanisms (Zink, 2002; Weiner, 1995). Using this widely accepted evolutionary model, it would be appropriate to say that phenotypic frequencies of avian populations are highly reactive to climate change.

1.1 AVIFAUNAL EVOLUTION

When investigating evolutionary habits of birds, it’s worth noting what record we have on their origin when predicting evolutionary directions. All birds possess feathers, lack teeth, are digitigrade, have a reduction of bones, high metabolism, have specialized forelimbs, and generally are small in size. In fact, the vast majority of birds are under a kilogram and smaller than 50 centimeters in length (Proctor, pgs 13-16). The avian group overall is much more morphologically uniform when compared to mammals or reptiles.

When looking at the fossil record, avian assemblages leave much to offer, yet known fossils clearly indicate that bird evolution was very rapid during the late Mesozoic as well as early in the Cenozoic. Late Cretaceous timing of angiosperms proliferation and the development of grasses in the Cenozoic no doubt produced an abundant supply of foods for birds to exploit and diversify through radiation. The reverse trend occurred later during the Pleistocene however. At the beginning of the Pleistocene epoch there may have been over twice as many bird species as there were at the end of the epoch. The Pleistocene is chiefly characterized by a time of great climatic instability, the likely culprit to the decimation of many species (Brusatte, 2015).

1.1.1 GEOGRAPHICAL CLINES IN MODERN AVIFAUNA

According to evidence of previous studies of modern birds, one might expect a marked morphological deviation during a Pleistocene climatic cooling cycle. Geographical clines are frequently reported in avian populations of a single species that inhabit extensive ranges, where the largest, most robust members are found in colder ranges while smaller, more limber members are found in warmer ranges. These latitudinal clines in body size and limb robustness are widely interpreted as evidence for natural selection and adaptation to local climate, and as such are predicted to shift during climate transitions (Gardner, 2009).

Allen’s and Bergman’s Rule

These types of clines support two basic evolutionary principles, Allen’s and Bergman’s rules (Symonds, 2010). Allen's rule proposes that relative to body size, the appendages of endotherms become smaller and stouter in cold climates; the reduced surface area increases heat retention. Bergman’s rule is a similar generalization as Allen’s rule, in that body size is said to be larger in populations that live in colder climates (Figure 1), also to reduce heat loss via a smaller proportion of exposed surface area.

In a study looking at the data of 94 species of birds, it was concluded that over 70% of the species had geographic clines, and did indeed follow Bergman’s rule, further supporting it to be a valid generalization for birds (Meiri, 2003). Rapid changes in avian body size correlating to climate change have also been identified in house sparrows, brown tree-creepers, grey-crowned babblers, hooded robins, yellow-rumped thorn bills, and variegated fairy-wrens in as little as 100 years (Mason, 2015). These previous studies on living bird populations support a hypothesis that climate change would catalyze morphological transition in birds, specifically size and limb robustness. However, based on current data, fossil studies do not tend to support this hypothesis.

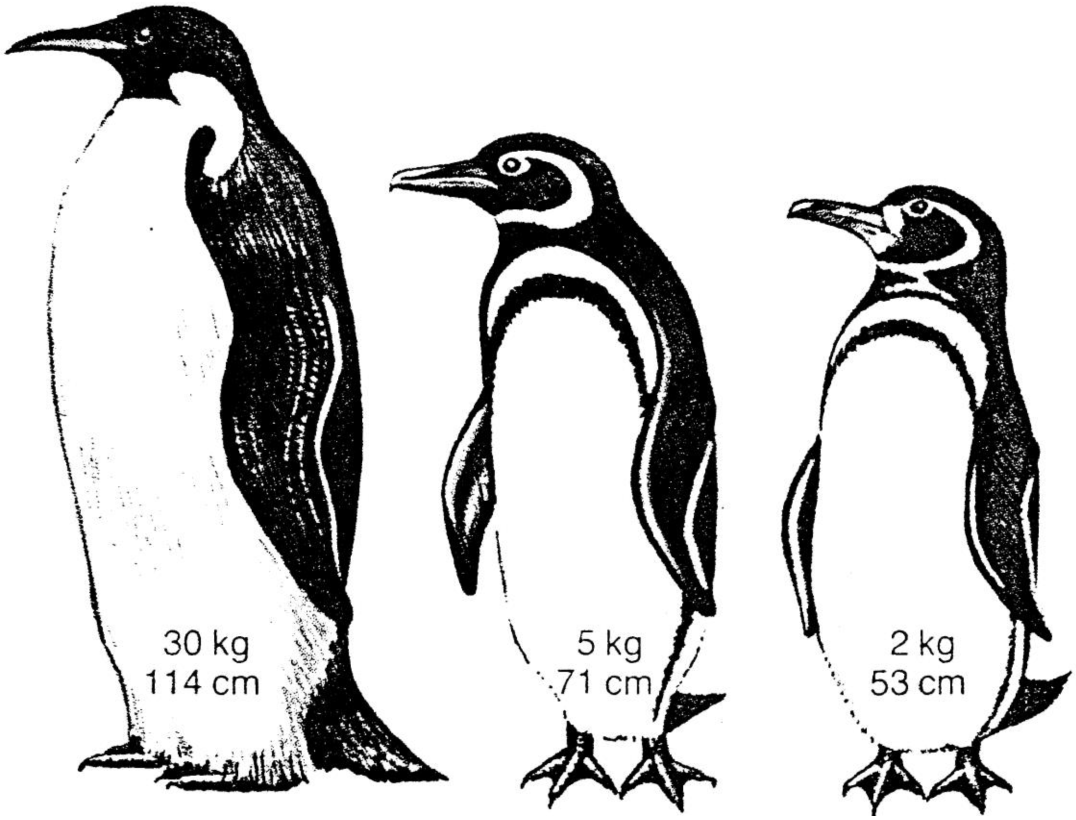

Figure 1*: Geographical clines in body size in penguin species. From left to right; Imperial (65S), Magellan (50S), and Galapagos Penguins (1 S). From (Pozdnyakov Vasilievich,, 2009; bio-faq.ru/zzz/zzz009.html*

1.2 - CONTROVERSY IN DARWINIAN MODELS: GRADULALISM VS. PUNCTUATED EQUILIBRIUM

Contrary to numerous studies correlating morphology to climate, the occurrence of phyletic gradualism, or gradual accumulation of adaptation through time, is rarely documented (Zink, 2002). In fact, most fossil animals show no change over millions of years (Gould, 2002). The phenomenon of stasis in such species contradicts gradualism (Figure 2), pointing to the theory that in fact most species are resistant to small-scale change over extended periods of time. Instead they change rapidly in short bursts between these periods of stasis. (Eldredge and Gould, 1972; Eldredge, 1999; Gould, 2002). This is true even through periods of climate change, which according to conventional evolutionary biology, should trigger obvious changes in size ormorphology. Eldredge and Gould (1972) called this model ‘Punctuated Equilibrium’ and deemed it an alternative to phyletic gradualism.

With these two opposing theories about morphological changes in response to climate change, it is worthwhile to analyze as many examples as possible. Investigations will help resolve the controversy and identify the variables that promote or refute the occurrence of stasis in bird species. Pleistocene specimens can demonstrate longer timespans of climate stress, making my fossil locality perfect for this study.

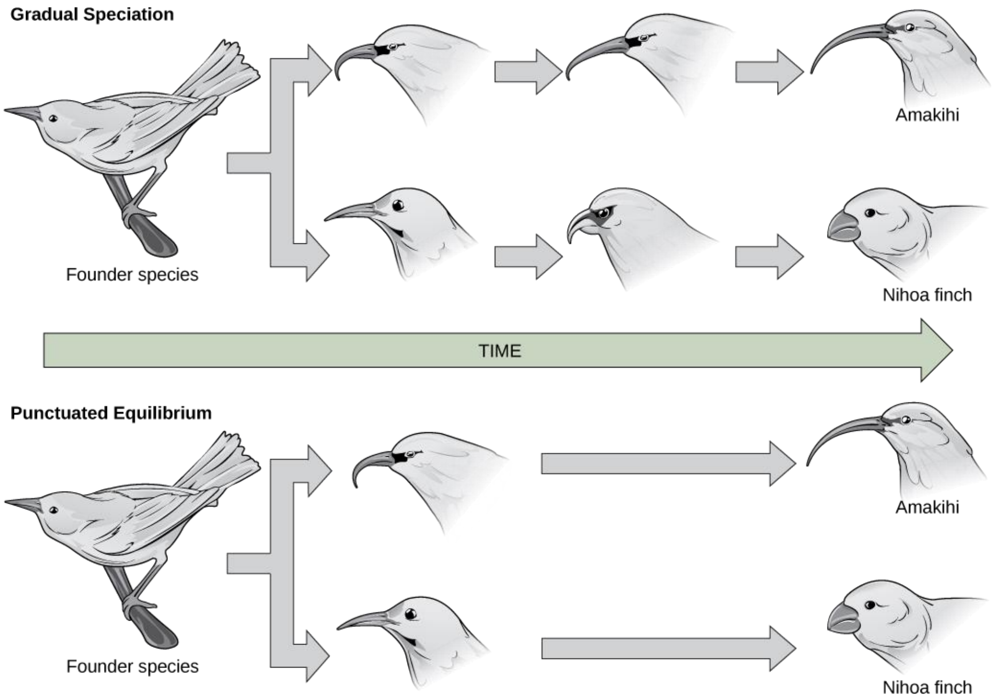

Figure 2: *Punctuated Equilibrium and Gradual Speciation are two opposing evolutionary models that predict appearances of species in the fossil record. Gradualism (top) illustrates the progressive change from one species to another. Although widely accepted, this is very rarely documented in fossil species. The more common phenomena illustrated (bottom) of punctuated equilibrium is often found in the fossil record, with a new species abruptly showing up after extended persistence of its parent species. From (Anshul Agrawal, 2017; https://www.quora.com/What-is-the-basic-difference-between-Speciation-and-evolution)*

1.3 RANCHO LA BREA

Rancho La Brea (RLB) tar pits, located in Los Angeles, California, are considered some of the most famous fossil deposits in the world, as it is a prominent area of research for Pleistocene animals in the region. Specimens can even be dated based on where they were retrieved from, since the locality is represented by multiple individual pits. This is because an active pit is made up of an asphalt ‘bubble’ that percolated up to the surface. During activity, they act as a sticky trap and often get reburied after some time, behaving as a natural ‘time capsule’. They can then be identified to correspond to specific late Pleistocene climate cycles based on radiocarbon dating of organics within (Marcus and Berger, 1984; O’Keefe et al., 2009).

Not only does RLB represent a well-dated animal fossil locality, but it also has well a well-defined vegetation history. Knowing vegetation makeup during climate statics is a crucial factor in evaluating historic ecosystems. Pollen records demonstrate changes from oak and chaparral vegetation at about 59 ka, to a pine, juniper, and cypress woodland at 24 ka, to a juniper-ponderosa forest about 20 ka, with significant snow even at low elevations like La Brea. From 14 to 10 ka, during the glacial-interglacial transition, the landscape returned to dominant oak-chaparral and coastal sagebrush, and since then the region has been populated by the modern assemblage of oak-chaparral-herbaceous vegetation (Heusser, 1998). RLB is a legendary Pleistocene locality, and its specimens prove that you can have both quality and quantity.

The pits to this day produce an outstanding number of fossils in superb condition. Fossil birds, which normally have relatively low preservation values, makeup 85,000 individual specimens at RLB. As of the last census, the specimens represent at least 114 extant species and 19 extinct species (Howard, 1962). The exquisite preservation of avian elements can be attributed to the properties of the asphalt itself. The asphalt served two important purposes: entrapment and preservation. Asphalt in the pits cushioned and sealed away its captives, allowing us to expose beautifully preserved delicate elements, like avian bones, that are normally degraded or destroyed (Akersten et al., 1983; Coltrain, 2004; Stock and Harris, 1992). The wealth of information that RLB yields makes it an excellent location to test a hypothesis on morphological adaptations in birds in response to environmental change over a timescale of several thousands of years, including through that last glacial-interglacial cycle at 14-10 ka (Coltrain, 2004; Madan, 2015).

1.3.1 PREVIOUS WORK

Pleistocene fossil records of Golden Eagles (Molina and Prothero, 2011), California Condors (Syverson and Prothero, 2010), Great Horned Owls (Madan and Prothero 2015), Barn Owls (Madan and Prothero, 2015), Bald Eagles, Turkeys, and Caracaras (Fragomeni and Prothero, 2011) retained body size and limb robustness throughout a climatic cooling cycle at Rancho La Brea. The most popular explanation for the stagnant morphology is that when an organism lives in large geographic ranges, they tend to be adapted to diverse environments and thus are resistant to local changes in climate. For this reason, when climate change occurs in their range, they don’t respond to it via changes to their morphology (Eldredge, 1999; Lieberman and Dudgeon, 1996; Eldredge et al., 2005). Interpretations of body size as a variable have yet to be investigated, it could be argued that smaller birds (like finches) should more sensitive to fluctuating microenvironments and more likely to change in response to climate change than large birds, which are spread over much larger geographic ranges with broader environmental differences. Since the previously studied birds at La Brea are extensively larger than reported responsive species (Finch, Sparrow etc.), more research is required.

1.3.2 PREVIOUSLY UNSTUDIED SPECIES

Species useful for investigating morphological divergences through La Brea time records must have measurable element proxies common in well dated pits. Museum records of inventoried avian collections reveals four candidate species previously not investigated.

Coragyps occidentalis

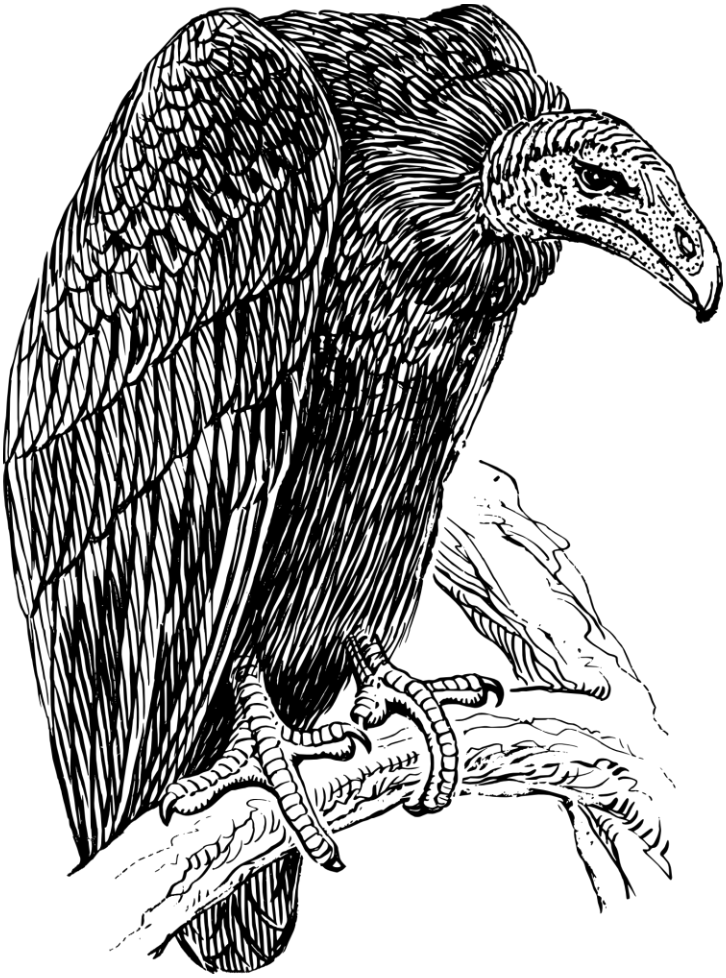

Figure 3: *Coragyps occidentalis; Western Black Vulture weighs approximately 2 kg, and its extinct relative would have been slightly larger, and overall represents the largest member in this study. C. occidentalis would be highly dependent of carrion as a food source just like their modern relatives, which may have played a factor in their extinction.*

The extinct Western Black Vulture *Coragyps occidentalis*, is best represented by a modern relative Black Vulture, *Coragyps atratus* (Figure 3*)*. Previously grouped with raptors such as hawks and eagles, the genus *Coragyps*, was found to be more closely related to storks after genetic testing. They are solitary, but sometimes travel in small groups. They are usually seen soaring on thermals at high altitudes, looking for carrion. (Sibley, pgs 94, 96).

Corvus corax

Figure 4: *Corvus corax; Common Raven weighs approximately 1.2 kgs, and represents the largest of three Passeriformes, or perching birds, included in this study (Black Vulture is not a passeriform). They are highly successful as they are a common in the US and Canada. Their high intellect and adaptability no doubt has played a role in their persistence through the fossil record.*

The Common Raven, *Corvus corax,* (Figure 4) is the largest of Passerines (perching birds), and the second largest member of this study, weighing in 1.2 kilograms. The highly intelligent bird is found in a wide array of habitats including tundra, forests, arid brush lands, coast lines, canyons, and mountainous regions. Its diet is variable as well, using a heavy bill to feed on small animals, bird eggs, snails, insects, seeds, fruits, and even human refuse (Davis pg 209, Sibley pg 309).

Pica nutalli

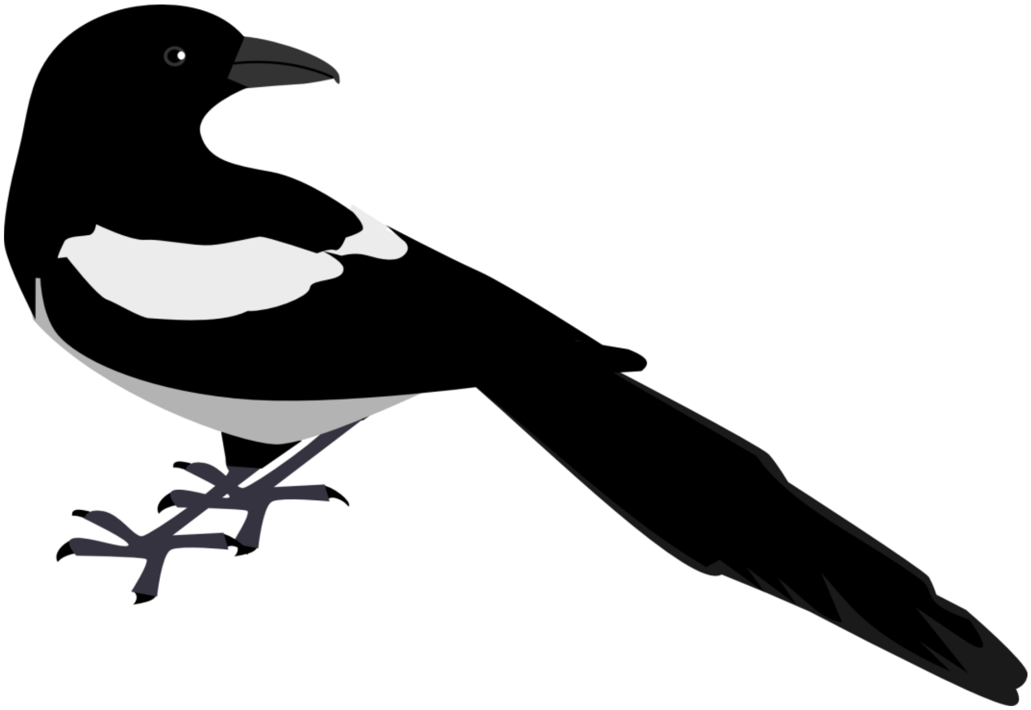

Figure 5: *Pica nutalli; Yellow-billed Magpie is rarely recorded outside of California, and spends much of its time on the ground, foraging for food. This feeding behavior probably what makes it common in RLB fossil deposits.*

Yellow-billed Magpie, *Pica nutalli*, (Figure 5) weighs about 155 grams thus represents the second smallest member of this study. It is common in oak savannas feeding on a variety of seeds and animal prey, foraging mostly on the ground. (Sibley pg 307). This species makes a good comparative model between the adaptable Raven and the year-round Western Meadowlark.

Sturnella neglecta

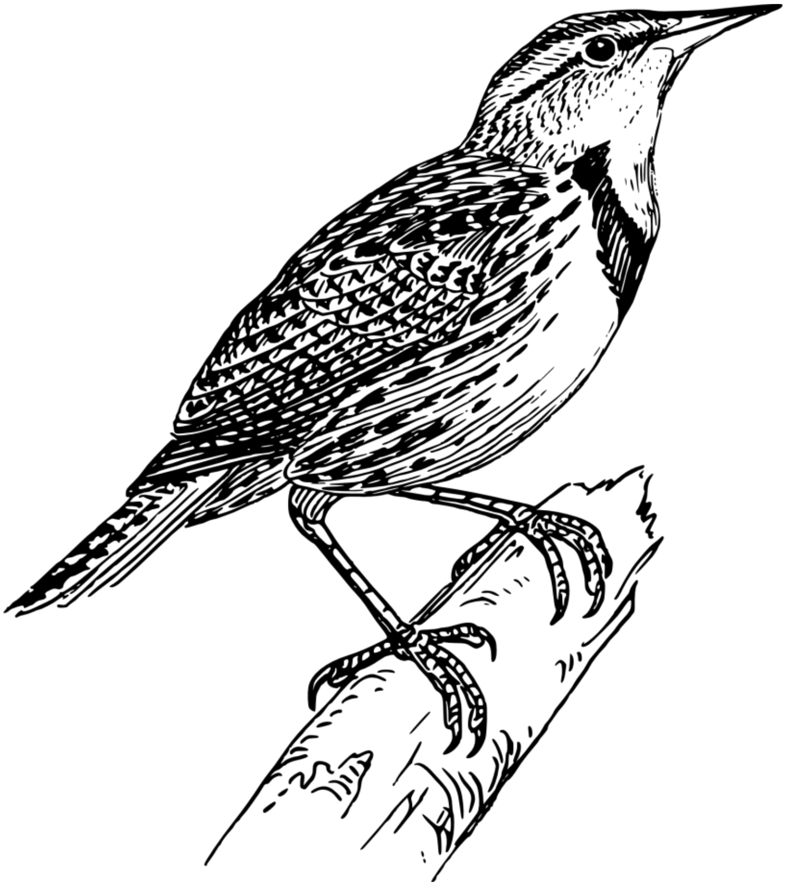

Figure 6. *Sturnella neglecta; Western Meadowlark is the smallest member of this study. In my study, Meadowlarks are most easily compared to finches due to their small size and their position in a similar ecological niche.*

Western Meadowlark, *Sturnella neglecta* (Figure 6) weighs on average about 97 grams. It is common in arid grasslands and feeds on seeds insects and worms and is found year-round in western U.S. (Sibley, pg 438). Meadowlarks nest in tall dry grass, lay 3-5 eggs on the ground a season and incubate for 13-15 days. They are land passerines and have well-developed legs for ground mobility. They feed on grasshoppers, cutworms, boll weevils, crickets, and other insects, while supplementing diet with a small amount of grain (Davis, pg 280).

1.4 – STUDY GOALS

For this study, I will attempt to identify any significant deviations of body size or limb proportions in Black Vultures, Meadowlarks, Raven, and Magpies at RLB over the last glacial and interglacial cycle by examining relevant specimens and modern relative specimens. Changes or lack thereof will be used in the discussion of the variable of adult body size as a factor to climate responses in the phenotypes of avifaunal populations. Based on the evolutionary principles of Bergman's and Allen's rule, as supported in modern avian populations through geographic clines and examples of rapid climatic avian adaptation in multiple studies, I expect that studied specimens will follow them as well. Specimens are specifically expected to have larger more robust proportions during glacial periods, while becoming smaller and more limber in warmer periods.

CHAPTER 2 - METHODOLOGY

Methodology was mainly based off previous RLB studies, with minor modifications to maximize sample sizes. The most commonly preserved element of the avian skeleton is the tarsometatarsus (TMT), which has been used as a proxy for body size in previous RLB bird studies and is one of the most abundant datasets available. TMTs are highly fused bones in the lower leg of all birds and are commonly preserved due to it their robustness. For these reasons, the use of TMTs will be continued in this study.

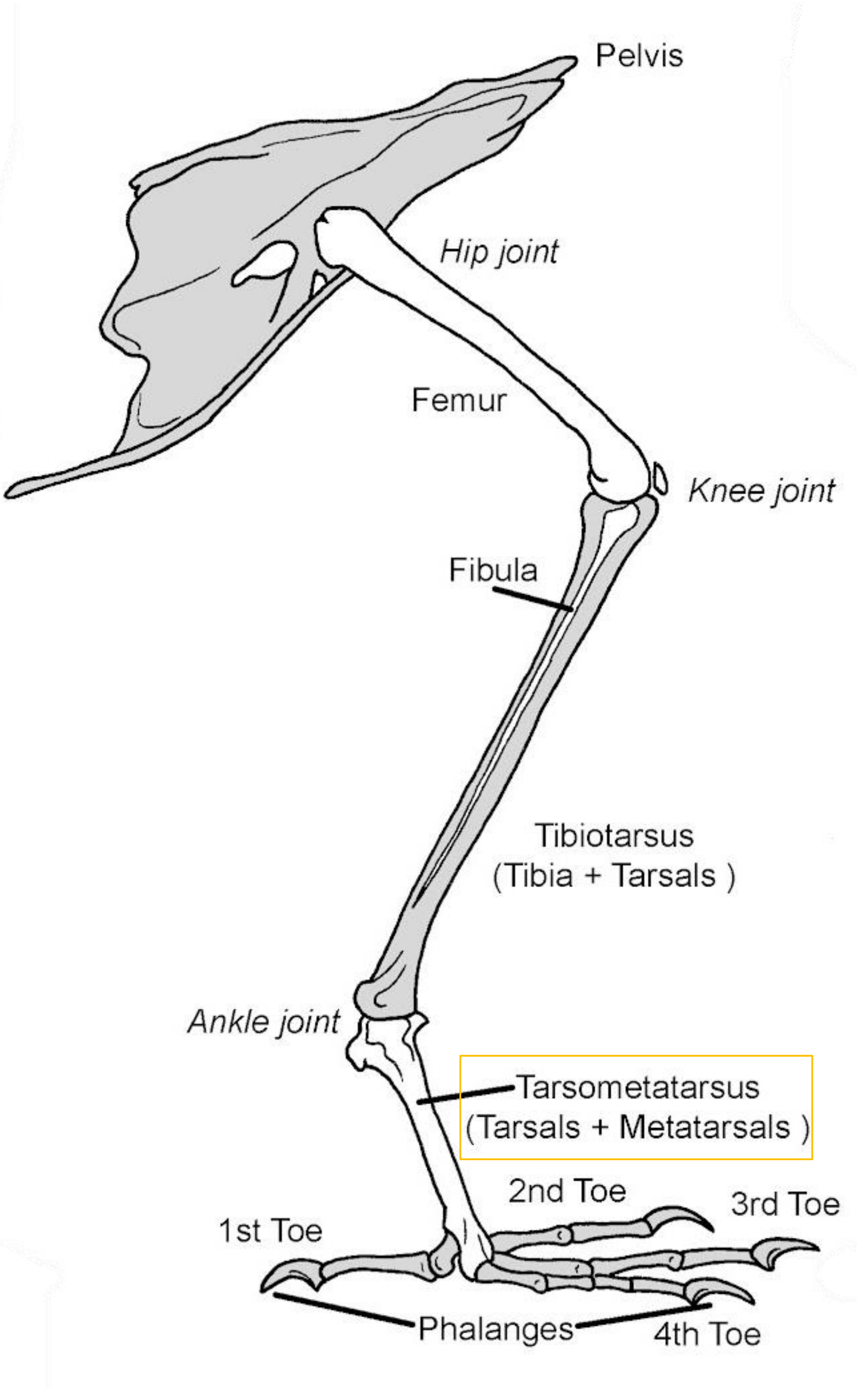

Figure 7*: Chicken leg anatomy. All birds possess the tarsometatarsus, a fused bone in the lower leg used as a lever of strength. The robustness of TMTs allow it to be useful in this study. From (2018;https://www.hdanatomy.com/anatomy-of-a-chicken-leg-for-interactive/)*

First, species candidates for the study were reviewed and chosen based on how common TMTs were found in well-dated pits. Based on knowledge of useful pits, and a census provided by museum staff, I found that *Coragyps occidentalis, Corvus corax, Pica nutallii,* and *Sturnella neglecta* were the only common small birds available for this study. The tarsometatarsus, TMT, is used across all four investigated species to reflect body size and limb proportions. (Syverson and Prothero, 2010).

2.1 – USING THE RLB COLLECTIONS

The RLB avian collections are organized via skeletal elements for each species. Although this organization allowed for quick retrieval of TMTs, it required catalog search for the data for each individual specimen. This was necessary to retrieve the information on which pit the TMT had been recovered from, so that I may only include well dated specimens. I excluded specimens in my sampling that came from pits like Pit 16, due to its widely scattered radiocarbon ages. Specimens coming from pits like these can confuse time-sensitive studies (Marcus and Berger, 1984; O'Keefe et al., 2009). Each species included several sample sets, only distinguished by age via pit origin.

2.2 – DATA COLLECTION

I measured adult TMTs with intact bone shafts (Figure 8), from well-dated pits, and identified within the collections as *Coragyps occidentalis, Corvus corax, Pica nutalli,* and *Sturnella neglecta*. Each specimen was measured with metric calipers, in three dimensions: maximum shaft length between the foramen beneath each epiphysis; mid-shaft transverse width; and mid-shaft anteroposterior thickness of the TMT. Modern specimens including Black Vulture relative (*Coragyps atratus)*, Magpie (*Pica nutalli*), Raven (*Corvus corax*), and Western Meadowlark (*Sturnella neglecta*) were measured at the Museum of Vertebrate Zoology at the University of California, Berkeley, and the Department of Ornithology at the American Museum of Natural History in New York. Modern specimens are noted as sample "0" in data.

Various assumptions are also made to streamline analysis including the following: specimens coming from the same pit come from the same population at averaged carbon-dated age; a TMT represents one individual; sexual dimorphism is negligible and/or averaged out; museum species identification is accurate; and specimens represent healthy non-pathological adult individuals.

2.3 – STATISTICAL ANALYSIS

The measurements were used to calculate two derived values as previously used in similar studies including; midshaft area (width x depth) and robustness index (midshaft area/length). The samples will be organized via age and will be evaluated for significant differences in each parameter (length, width, depth, midshaft area, and robustness index) on a per species basis. The statistical test used is a non-parametric Kruskal-Wallis test with pooled variance (as the distributions will be non-normal due to a skew in available well dated pits from which specimen ages will be derived). XLSTAT software was utilized for analysis.

The computed p-value is compared to the significance level alpha=0.05. When P-values are computed above the significance level, I accept the null hypothesis. The null hypothesis, H_o, states that all the samples come from the same population. Our alternative hypothesis, H_a, states that the samples do not come from the same population, in that significances are found amongst samples. H_a will be accepted when the computed p-value falls below the significance level. Dunn's procedure is simultaneously utilized in XLSTAT as a multiple pairwise comparison tool, so that if significance is detected after Kruskal-Wallis analysis, divergent samples can be singled out.

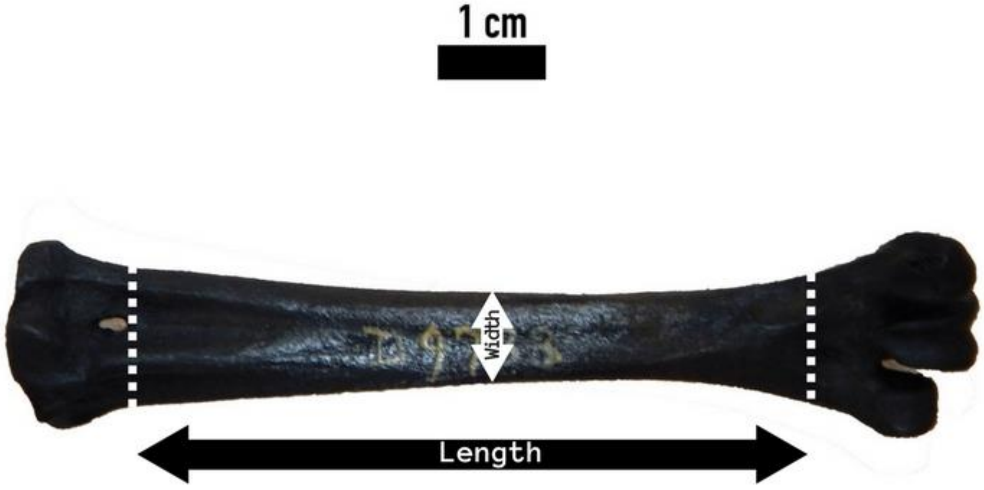

Figure 8: *Coragyps occidentalis TMT shown measured below foramen for length. As opposed to previous studies, where lengths are taken including the epiphysis. Measuring adult TMT's in this manner allowed the use of specimens with broken Epiphysis, thus expanding my dataset.*

CHAPTER 3 – RESULTS/DISCUSSION

3.1 BLACK VULTURE

Table 1. *Coragyps occidentalis*, Black Vulture summary statistics

Parameter	***Age(ka)***	***N***	***Minimum***	***Maximum***	***Mean***	***SD***
Length	**0**	**36**	**51.444**	**62.656**	**58.761**	**1.999**
	14	**92**	**50.700**	**61.100**	**56.799**	**2.258**
	18	**60**	**50.100**	**66.900**	**56.330**	**2.985**
	21	**13**	**55.500**	**59.300**	**57.377**	**1.137**
	35	**9**	**52.300**	**59.500**	**56.211**	**2.116**
Width	**0**	**36**	**6.000**	**9.600**	**7.564**	**0.976**
	14	**92**	**6.300**	**9.000**	**7.327**	**0.574**
	18	**60**	**6.400**	**9.000**	**7.515**	**0.554**
	21	**13**	**6.400**	**8.300**	**7.308**	**0.539**
	35	**9**	**6.800**	**9.000**	**7.689**	**0.666**
Depth	**0**	**36**	**4.400**	**7.500**	**6.086**	**0.762**
	14	**92**	**4.600**	**6.600**	**5.573**	**0.443**
	18	**60**	**4.700**	**6.500**	**5.615**	**0.438**
	21	**13**	**5.000**	**6.200**	**5.615**	**0.395**
	35	**9**	**5.000**	**6.800**	**5.667**	**0.515**
Midshaft Area	**0**	**36**	**27.280**	**70.500**	**46.584**	**10.863**
	14	**92**	**30.550**	**59.400**	**40.940**	**5.512**
	18	**60**	**31.850**	**58.500**	**42.317**	**5.568**
	21	**13**	**34.680**	**51.460**	**41.109**	**4.998**
	35	**9**	**35.000**	**61.200**	**43.782**	**7.463**

Table 1. Continued

Parameter	***Age(ka)***	***N***	***Minimum***	***Maximum***	***Mean***	***SD***
RI	0	36	0.485	1.252	0.794	0.193
	14	92	0.525	1.021	0.722	0.098
	18	60	0.565	0.995	0.752	0.097
	21	13	0.598	0.898	0.717	0.089
	35	9	0.629	1.044	0.779	0.124

Kruskal-Wallis analysis determined significance in length, depth, midshaft area, and robustness (Figure 9) in *Coragyps* spp. (*C. occidentalis* + *C. atratus*). Multiple pairwise comparisons using Dunn’s procedure along with Bonferroni’s correction identified the significantly different group to be attributed by sample set ’0’, measured from modern specimens of *Coragyps atratus*. *Coragyps occidentalis* and *Coragyps* atratus did not come from the same population. When *C. atratus* (modern representative for extinct *C. occidentalis*) was removed and the analysis run again, the results changed (Figure 9). No significant differences were detected between any of the Pleistocene samples of extinct Black Vulture in the different RLB pits, indicating stasis in the species. Spearman Correlation statistics were run on the sample as a check on initial results. Correlation results matched initial results indicating no significant size deviations in any of the RLB samples.

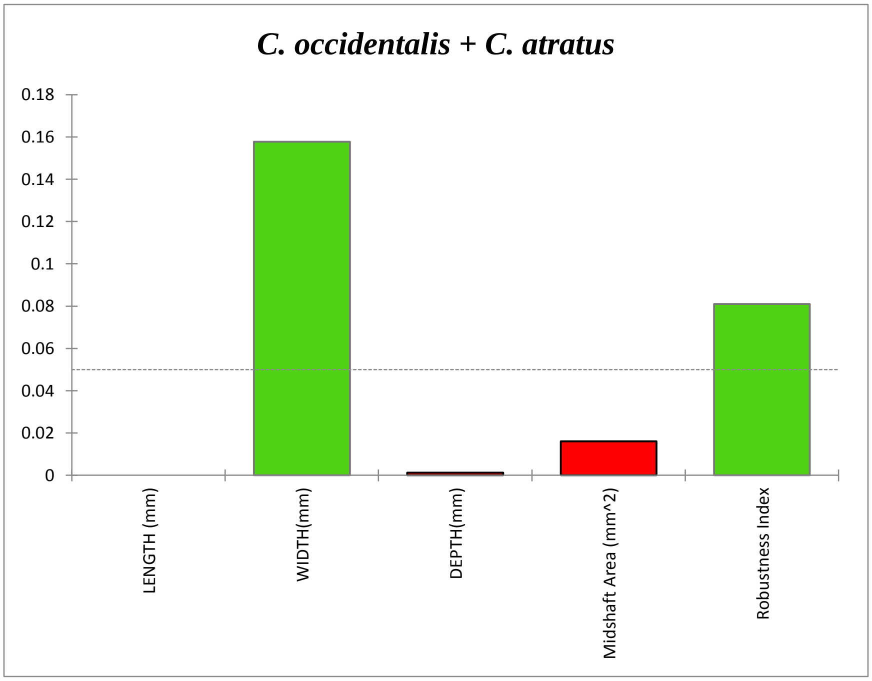

Figure 9: *Kruskal-Wallis p-values for extinct black vulture and modern black vulture (above). P-values less than 0.05 indicate significance in length, depth, and midshaft area. When computed without modern relative (bottom), no significance is detected*

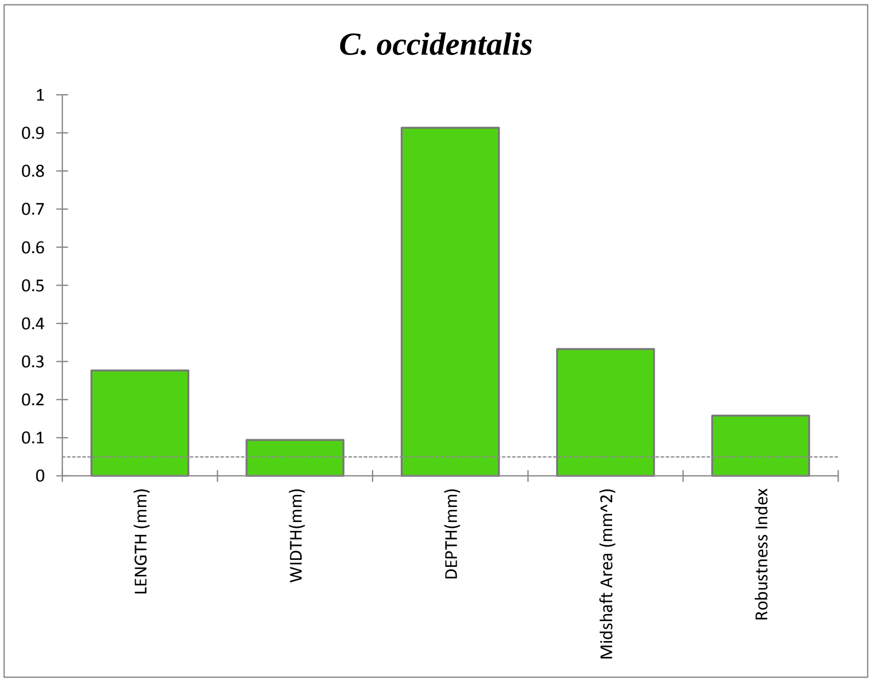

It’s clear that there are significant differences between the extinct Western Black Vulture and the modern Black Vulture (Figure 15), which is not particularly surprising. Although likely a single phylogenetic line, it’s not completely clear if the *C. occidentalis* evolved into *C. atratus*, or they’re completely distinct species altogether. In either case, Western Black Vulture resists any significant morphological changes during the most drastic climate events at RLB.

Figure 10. *Scatter plot of TMT observations from Black vulture. Lines intersect means. Age in ka along x axis. Modern sample displayed significance in length, depth, midshaft area, and robustness index (RI). Plots indicate that C. atratus is larger and less robust than fossil C. occidentalis.*

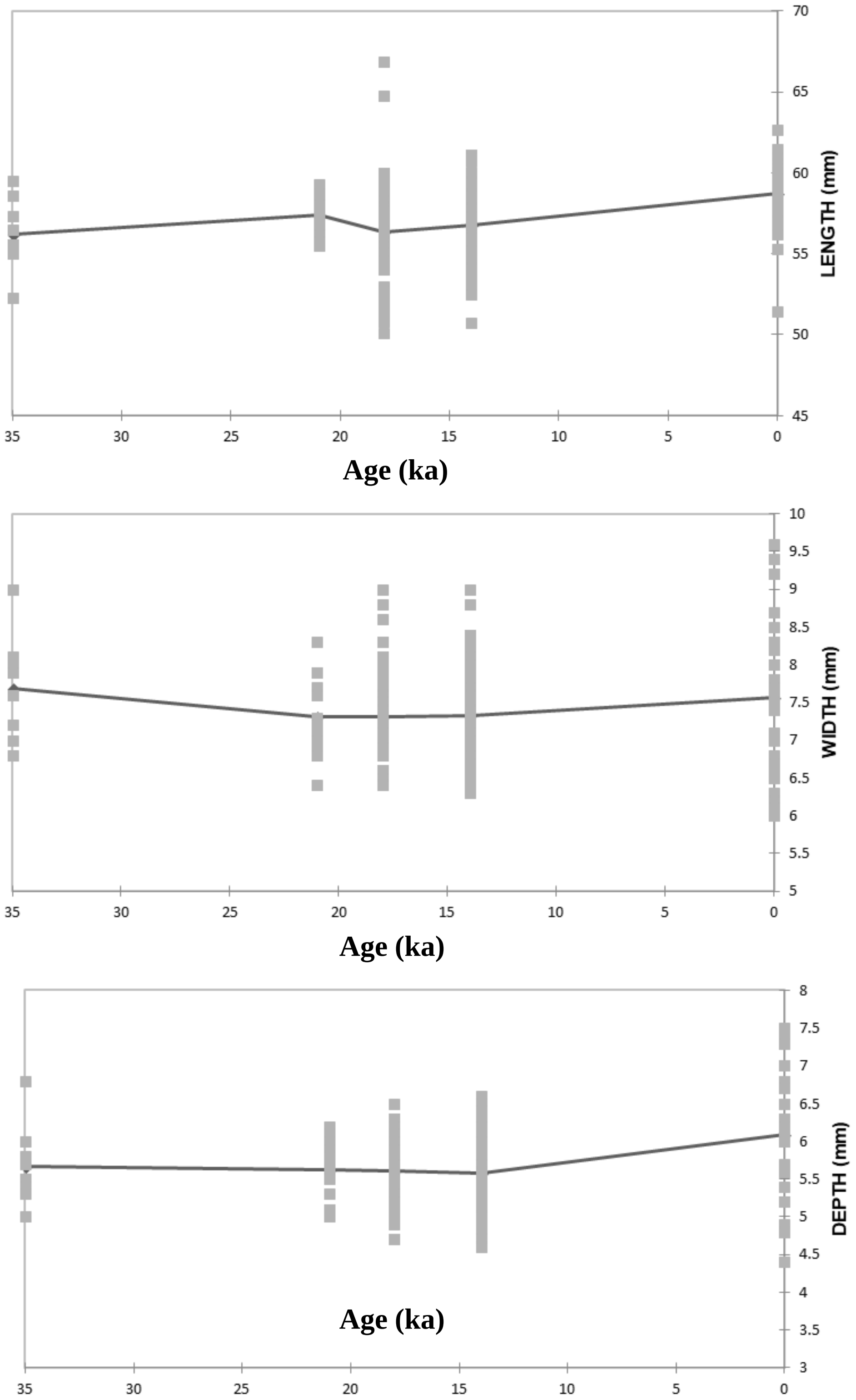

Figure 10. *Continued*

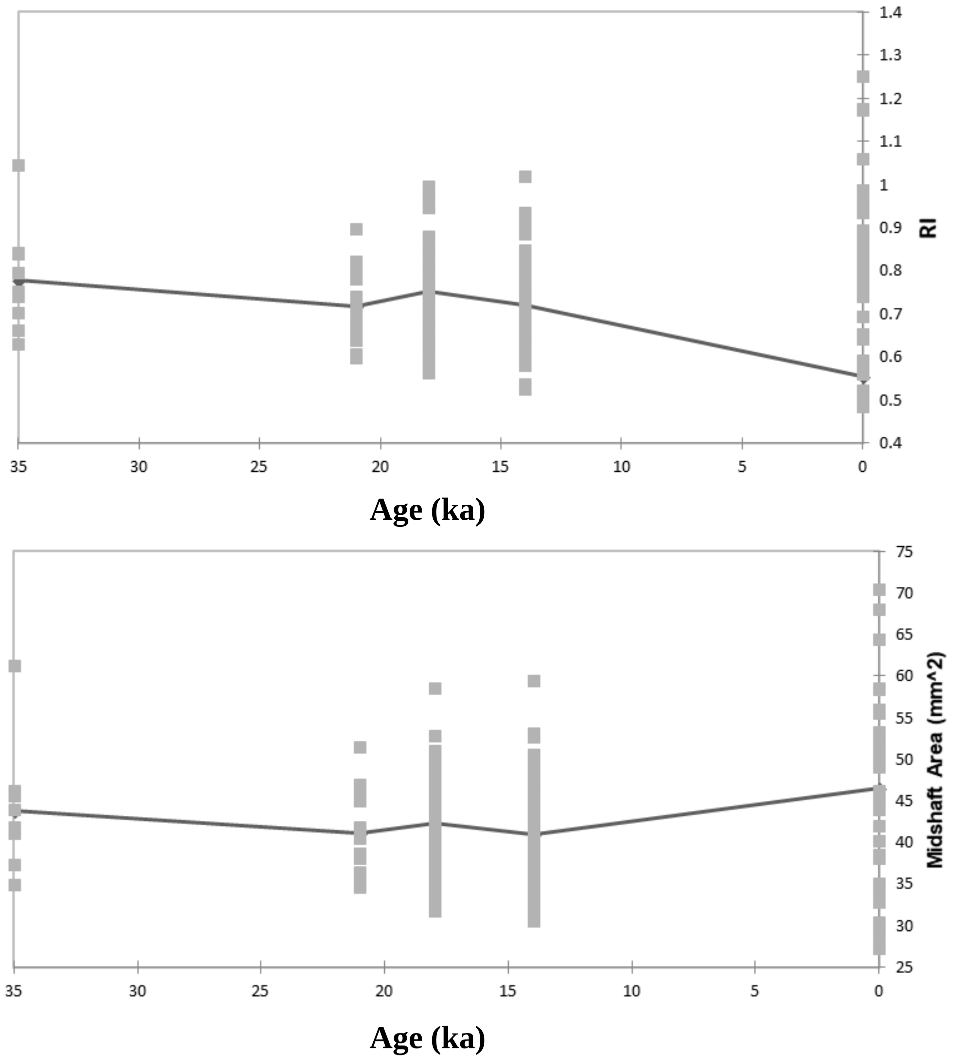

3.2 - COMMON RAVEN

Table 2. *Corvus corax*, Common Raven summary statistics

Parameter	*Age(ka)*	*N*	*Minimum*	*Maximum*	*Mean*	*SD*
Length	0	15	43.400	50.000	47.033	2.219
	9	81	40.300	52.200	46.098	2.459
	11	7	42.500	49.400	46.100	2.357
	14	32	42.000	50.800	45.859	2.216
	16	6	41.800	50.200	46.117	3.595
	18	14	43.600	51.000	46.286	2.069
	21	1	49.000	49.000	49.000	0.000
	29	9	39.600	58.300	45.156	5.667
Width	0	15	3.600	5.500	4.420	0.692
	9	81	3.100	5.700	4.209	0.464
	11	7	3.700	5.500	4.200	0.600
	14	32	3.600	5.700	4.075	0.406
	16	6	3.900	5.900	4.500	0.767
	18	14	3.500	5.000	4.021	0.426
	21	1	4.000	4.000	4.000	0.000
	29	9	3.600	4.600	3.978	0.311
Depth	0	15	4.500	6.000	5.113	0.487
	9	81	3.100	5.900	4.294	0.531
	11	7	3.300	4.600	4.114	0.438
	14	32	3.300	5.700	4.666	0.494
	16	6	3.500	5.700	4.867	0.819
	18	14	3.400	5.500	4.557	0.557
	21	1	4.900	4.900	4.900	0.000
	29	9	3.200	4.700	4.311	0.473

Table 2. Continued

Parameter	***Age(ka)***	***N***	***Minimum***	***Maximum***	***Mean***	***SD***
Midshaft Area	0	15	16.200	32.450	22.813	5.301
	9	81	10.850	31.350	18.143	3.455
	11	7	13.860	23.650	17.296	3.258
	14	32	13.680	27.360	19.005	2.735
	16	6	15.400	28.320	21.907	5.225
	18	14	12.240	27.500	18.456	3.798
	21	1	19.600	19.600	19.600	0.000
	29	9	12.480	21.620	17.158	2.425
RI	0	15	0.326	0.680	0.486	0.113
	9	81	0.255	0.620	0.393	0.067
	11	7	0.299	0.501	0.375	0.063
	14	32	0.292	0.553	0.415	0.057
	16	6	0.363	0.613	0.475	0.105
	18	14	0.266	0.539	0.399	0.079
	21	1	0.400	0.400	0.400	0.000
	29	9	0.313	0.432	0.380	0.034

Kruskal-Wallis analysis determined significance in the dimensions of depth, midshaft area, and robustness index. Multiple pairwise comparisons for *Corvus corax* identified the significantly distinct groups of all three parameters to be predominantly modern sample 0, but also identified significance in specimens at 9 and 11 ka for depth. Looking back at the raw data (Figure), it’s clear that modern specimens are larger when compared to fossil *Corvus corax*, while the sample at 9 ka appear to have a shallowest depth and the 11 ka sample follows thereafter.

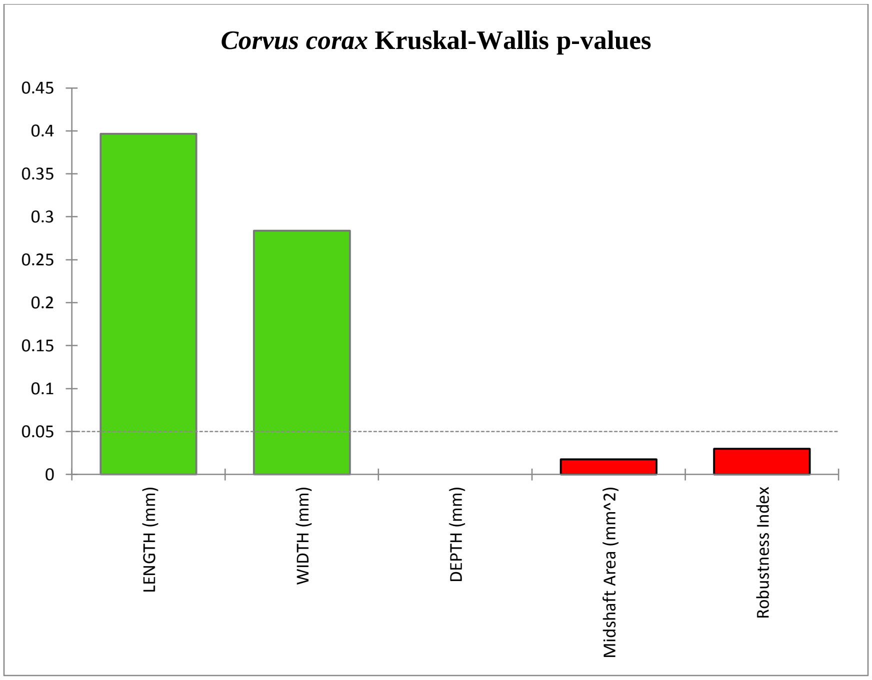

Figure 11. *Kruskal Wallis p-values for Common Raven including modern sample (above) and excluding modern sample (below). P-values less than 0.05 indicate significance in midshaft area and robustness index in modern sample and depth in both modern and fossil samples*.

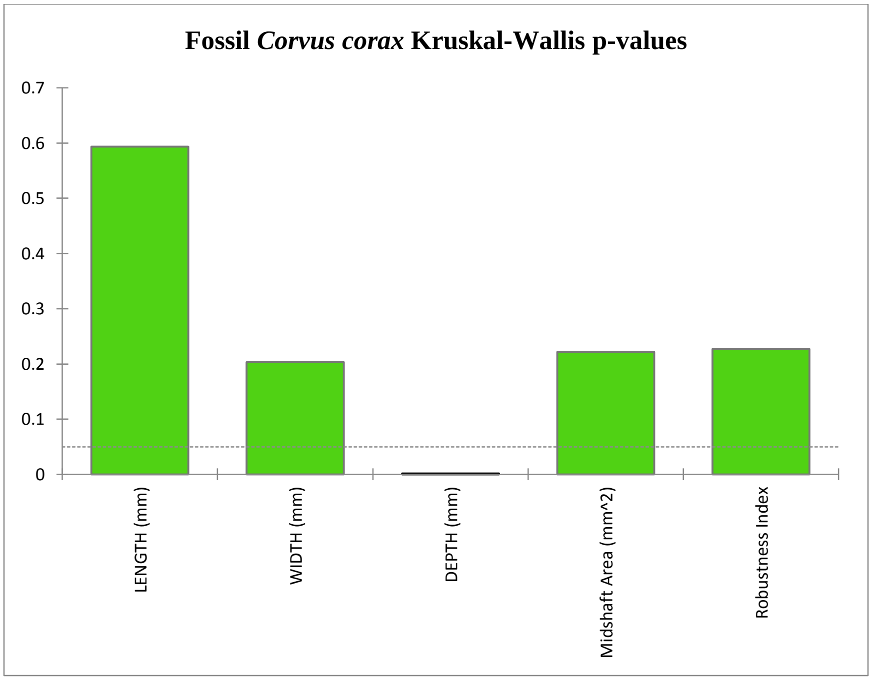

The appearance of the larger modern dataset opposes hypothetical trends. This species is commonly seen exploiting human refuse and urban areas, making an argument that anthropogenic dynamics may play a role in larger modern individuals after the Pleistocene, over climate change. Samples of *Corvus corax* at 9 and 11 ka do follow expected trends only in depth as climate warms and continued to trend this way thereafter. It’s unclear how significant this parameter is to the sample set, especially as it doesn’t appear significant enough to diverge midshaft parameters or robustness calculations (in which are both calculated from depth). From these results, I report stasis in *Corvus corax*, Common Raven at La Brea, but note that the variable of depth of TMT and its significance should be further investigated.

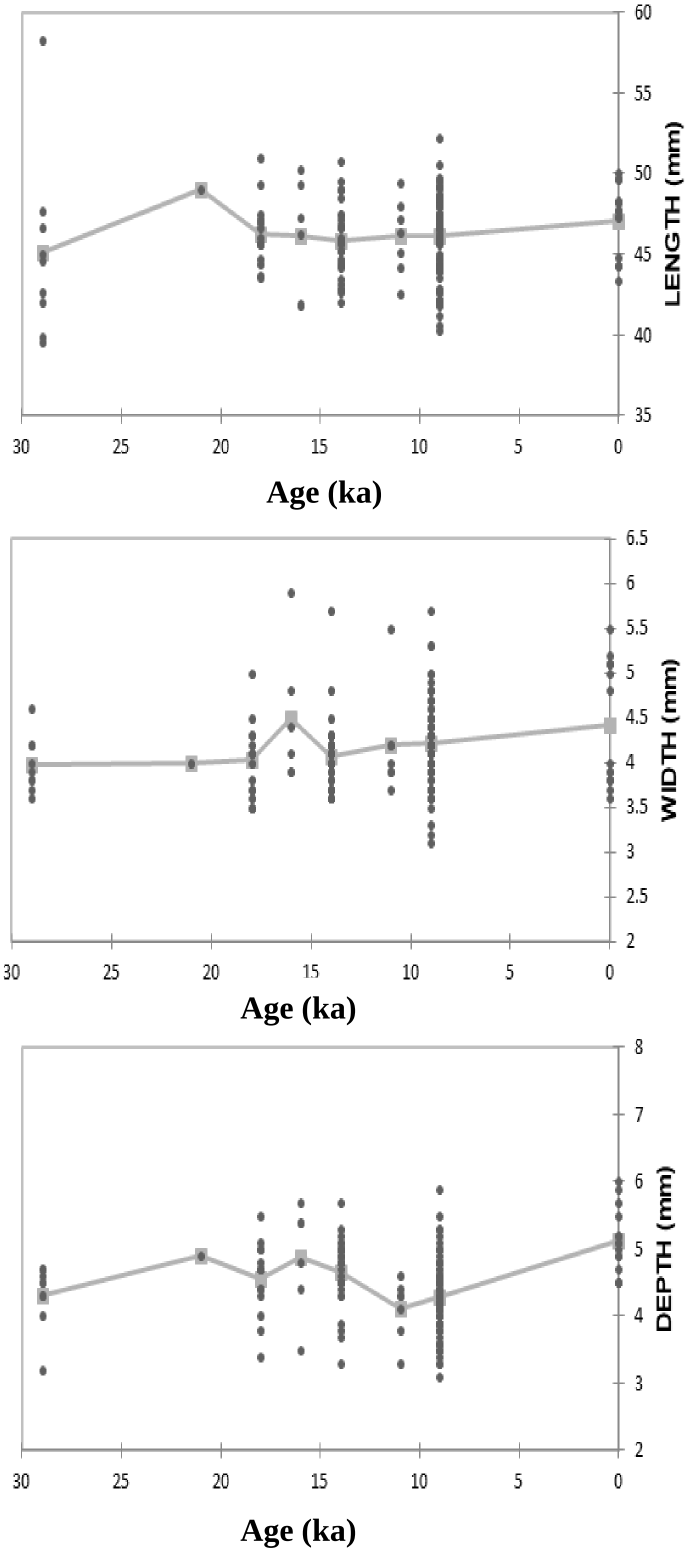

Figure 12. *Raven observations per parameter measured. X axis represents age in ka. Lines transect sample means. Kruskal-Wallis significance detected sample deviations in modern Corvus corax for depth, midshaft area, and robustness index, as well as 9 and 11 ka samples for depth.*

Figure 12. *(Continued)*

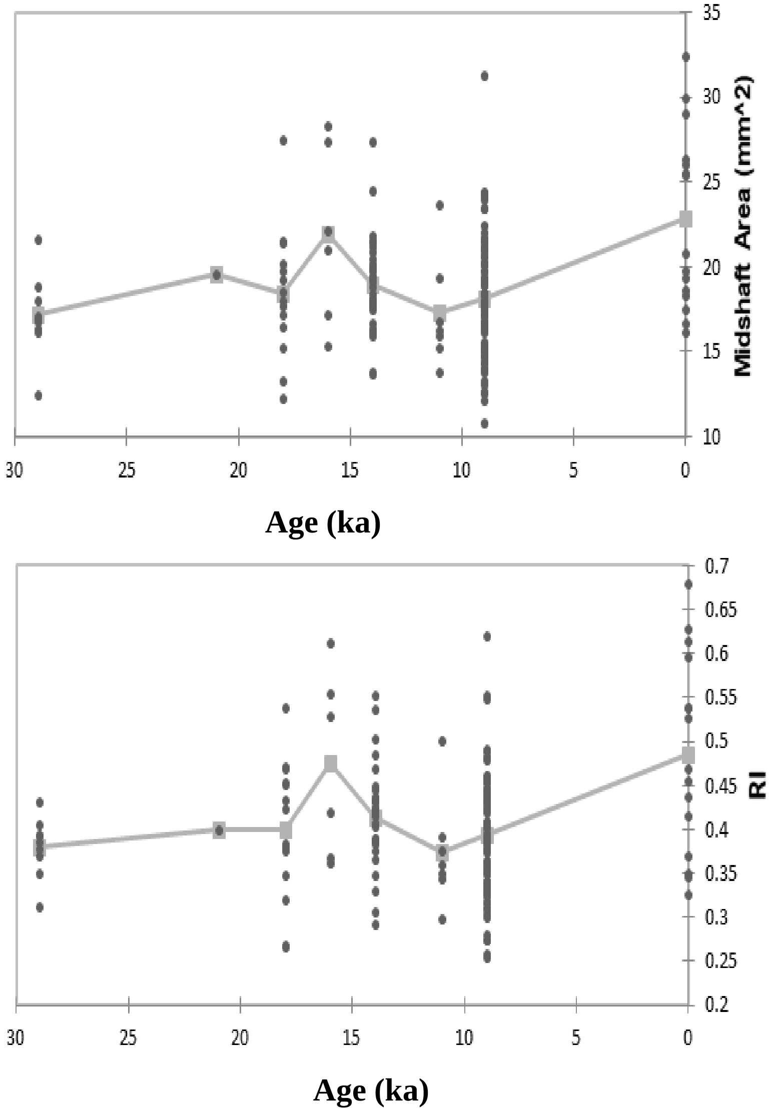

3.3 - YELLOW-BILLED MAGPIE

Table 3. *Pica nutalli*, Yellow-Billed Magpie summary statistics

Parameter	Age(ka)	N	Minimum	Maximum	Mean	SD
Length	0	13	33.075	42.300	36.513	2.611
	9	2	45.200	45.800	45.500	0.424
	11	2	46.400	47.100	46.750	0.495
	14	11	41.800	48.100	46.400	1.770
	16	3	46.800	49.300	47.733	1.365
	18	2	47.500	47.800	47.650	0.212
	29	1	43.200	43.200	43.200	0.000
Width	0	13	1.200	3.000	1.785	0.669
	9	2	2.100	2.500	2.300	0.283
	11	2	2.500	2.600	2.550	0.071
	14	11	2.200	2.900	2.500	0.228
	16	3	2.500	3.000	2.833	0.289
	18	2	2.400	2.400	2.400	0.000
	29	1	3.000	3.000	3.000	0.000
Depth	0	13	1.600	3.500	2.323	0.589
	9	2	2.500	2.500	2.500	0.000
	11	2	3.000	3.000	3.000	0.000
	14	11	2.400	3.600	2.809	0.333
	16	3	2.500	2.800	2.667	0.153
	18	2	2.800	3.100	2.950	0.212
	29	1	2.800	2.800	2.800	0.000

Table 3. Continued

Parameter	Age(ka)	N	Minimum	Maximum	Mean	SD
Midshaft Area	0	13	1.920	9.240	4.392	2.523
	9	2	5.250	6.250	5.750	0.707
	11	2	7.500	7.800	7.650	0.212
	14	11	5.750	9.000	7.008	0.939
	16	3	6.750	8.400	7.550	0.826
	18	2	6.720	7.440	7.080	0.509
	29	1	8.400	8.400	8.400	0.000
RI	0	13	0.054	0.260	0.123	0.075
	9	2	0.116	0.136	0.126	0.014
	11	2	0.159	0.168	0.164	0.006
	14	11	0.126	0.193	0.151	0.021
	16	3	0.137	0.179	0.159	0.021
	18	2	0.141	0.156	0.149	0.010
	29	1	0.194	0.194	0.194	0.000

Kruskal-Wallis analysis determined significance in length, width, depth, and midshaft areas in TMT of *Pica nutalli*. Multiple pairwise comparisons identified the significantly different group to be modern sample set of Yellow-Billed Magpies. When looking at observational data and means (figure), modern sample of Pica nutalli are much smaller.

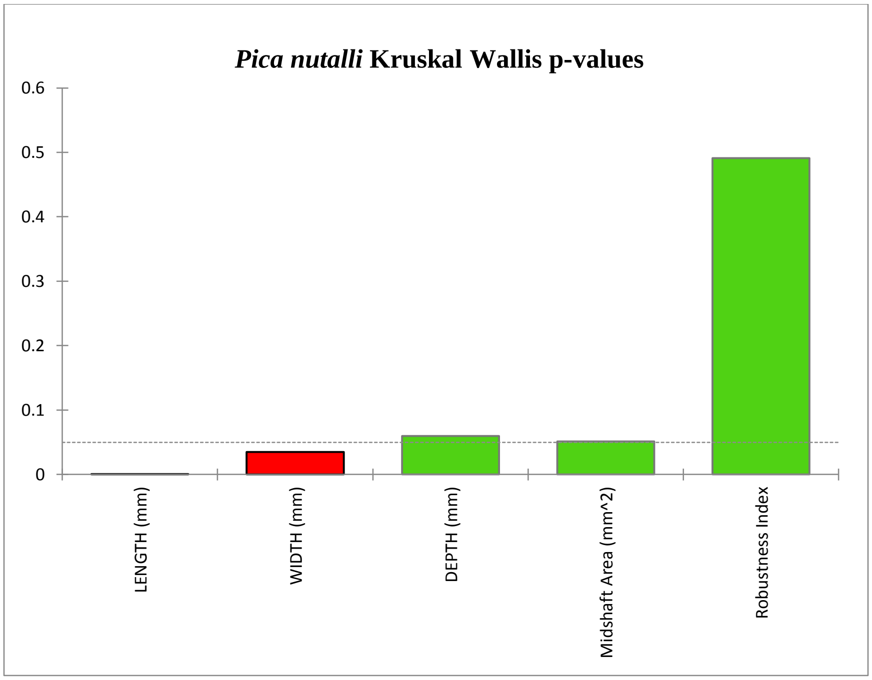

Figure 13. Kruskal-Wallis p-values for Yellow-Billed Magpie including modern sample (above) and excluding modern sample (below). P-values less than 0.05 indicate significance in TMT length and width in modern sample.

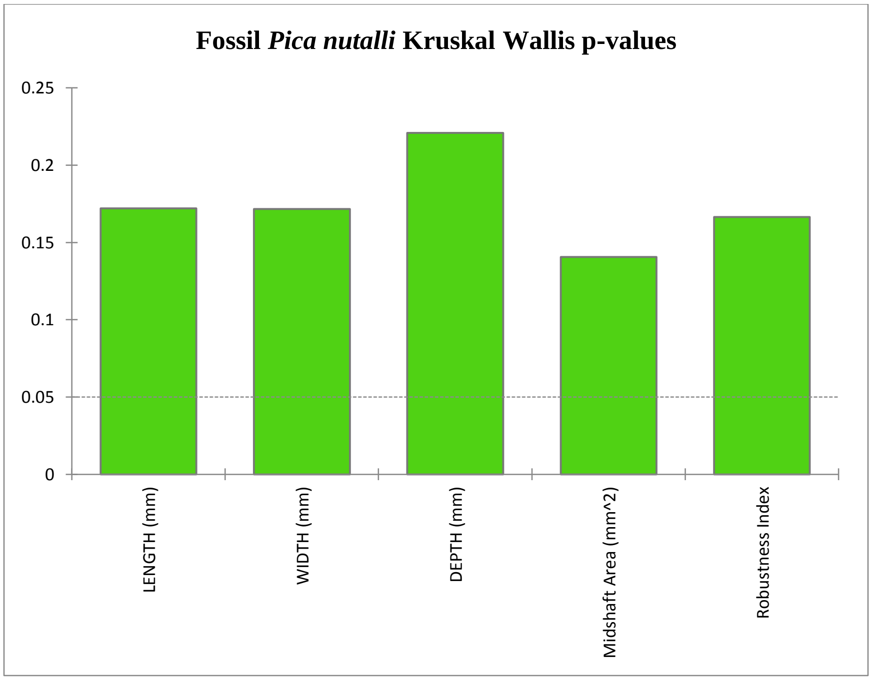

Results are congruent with hypothesis of climate warming and selection for smaller body size for Pica nutalli of modern against fossil species. However, the change occurs after the Pleistocene which contrasts gradualist trends. Retention of morphology up until this point exemplifies punctuated equilibrium, in which changes in species are marked in short bursts separated by extended periods of stasis. For these reasons, I report stasis in *Pica nutalli* through RLB Pleistocene records.

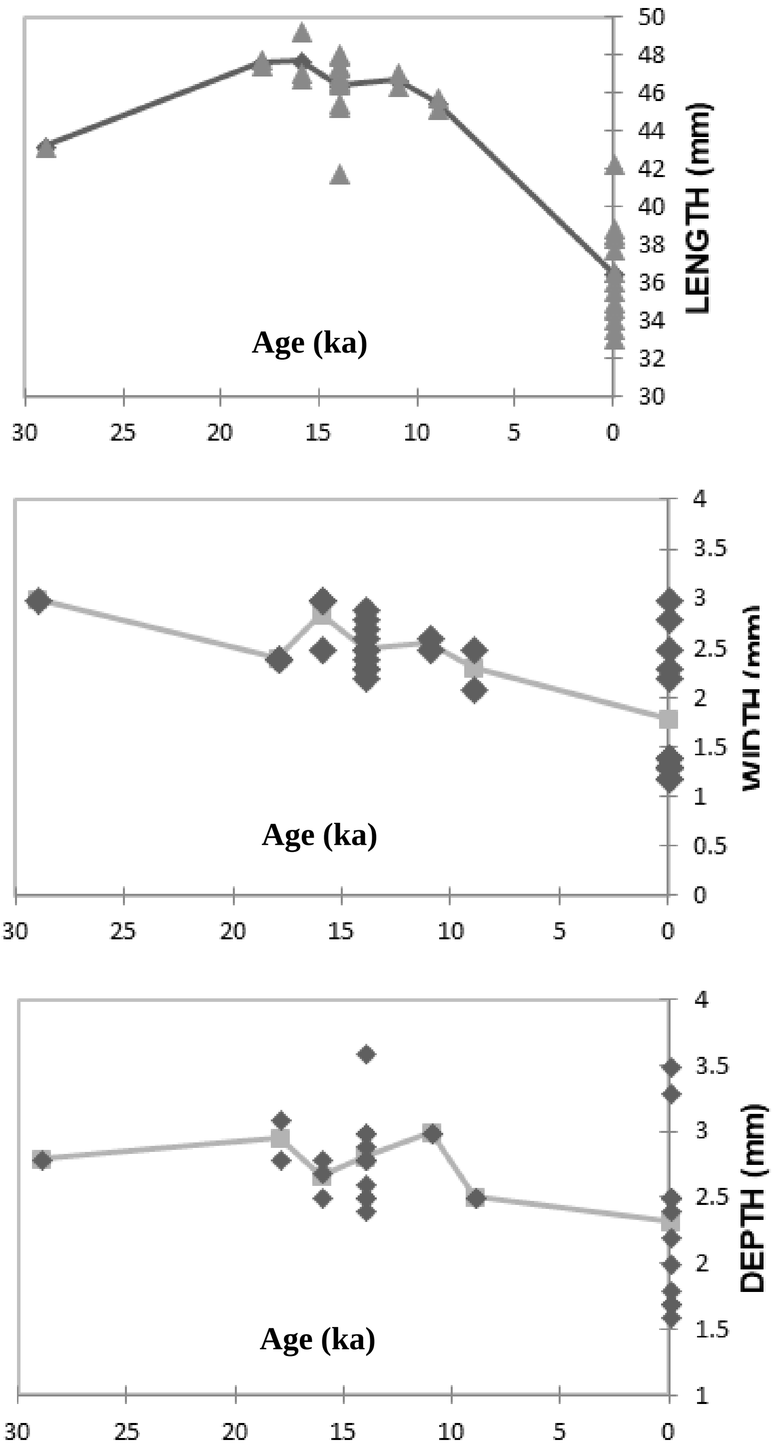

Figure 14. *Yellow-Billed Magpie observations per parameter measured. Horizontal axis represents age in ka. Lines transect sample means. Kruskal-0Wallis significance detected sample deviations in modern Pica nutalli for TMT length and width.*

Figure 14. *Continued*

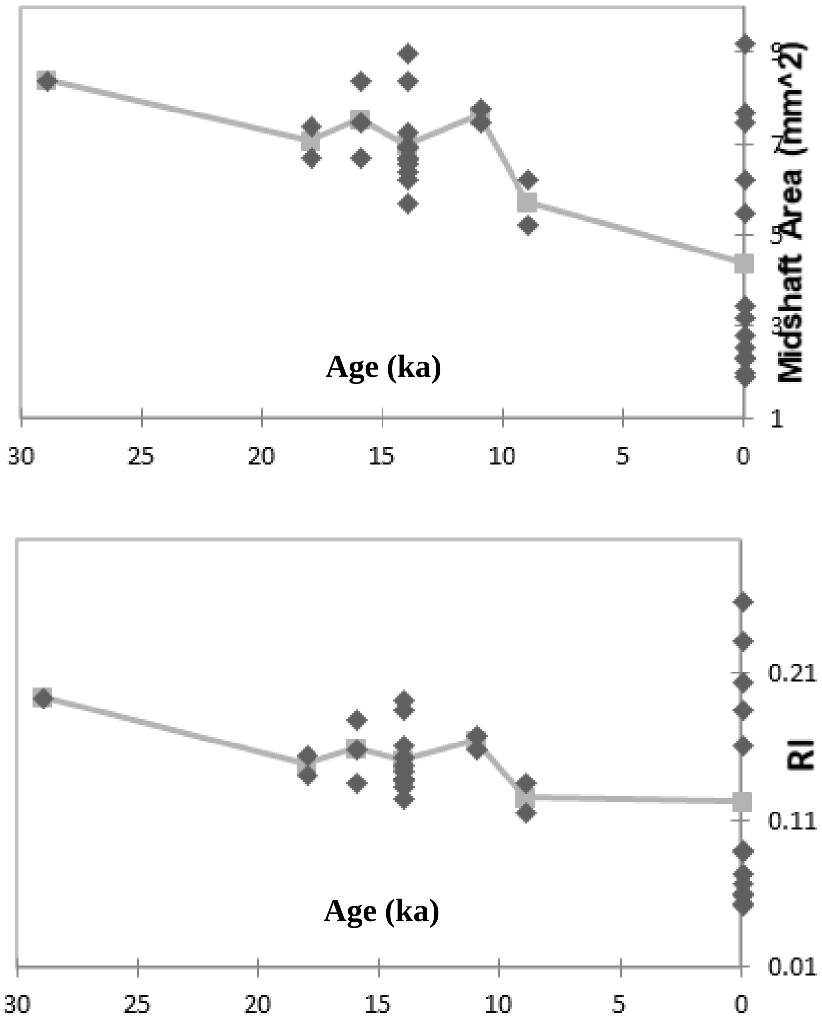

3.4 - WESTERN MEADOWLARK

Table 4. *Sturnella neglecta*, Western Meadowlark summary statistics

Parameter	***Age(ka)***	***N***	***Minimum***	***Maximum***	***Mean***	***SD***
Length	0	8	27.400	30.300	28.750	0.987
	9	15	36.100	39.500	38.007	1.164
	14	2	38.500	41.000	39.750	1.768
	18	6	34.500	39.300	36.917	1.724
	29	10	35.500	40.200	37.610	1.466
Width	0	8	0.800	1.700	1.125	0.320
	9	15	2.100	2.600	2.313	0.141
	14	2	2.300	2.600	2.450	0.212
	18	6	2.100	2.800	2.500	0.237
	29	10	2.000	3.000	2.510	0.292
Depth	0	8	1.000	2.100	1.650	0.325
	9	15	1.700	2.900	2.427	0.291
	14	2	2.100	2.700	2.400	0.424
	18	6	2.000	2.700	2.383	0.248
	29	10	2.300	3.100	2.580	0.305
Midshaft Area	0	8	1.100	2.940	1.861	0.681
	9	15	3.570	6.670	5.617	0.755
	14	2	4.830	7.020	5.925	1.549
	18	6	5.040	6.760	5.942	0.697
	29	10	5.000	8.370	6.498	1.205

Table 4. Continued

Parameter	***Age(ka)***	***N***	***Minimum***	***Maximum***	***Mean***	***SD***
RI	0	8	0.039	0.100	0.064	0.022
	9	15	0.096	0.180	0.148	0.020
	14	2	0.125	0.171	0.148	0.032
	18	6	0.142	0.180	0.161	0.016
	29	10	0.132	0.223	0.173	0.035

Kruskal-Wallis analysis determined significance in all parameters in *Sturnella neglecta*. Multiple pairwise comparisons identified the significantly different group to be attributed by sample set ’0’, measured from modern specimens of *Sturnella neglecta*. Observations of modern meadowlarks appear significantly smaller than fossil meadowlarks.

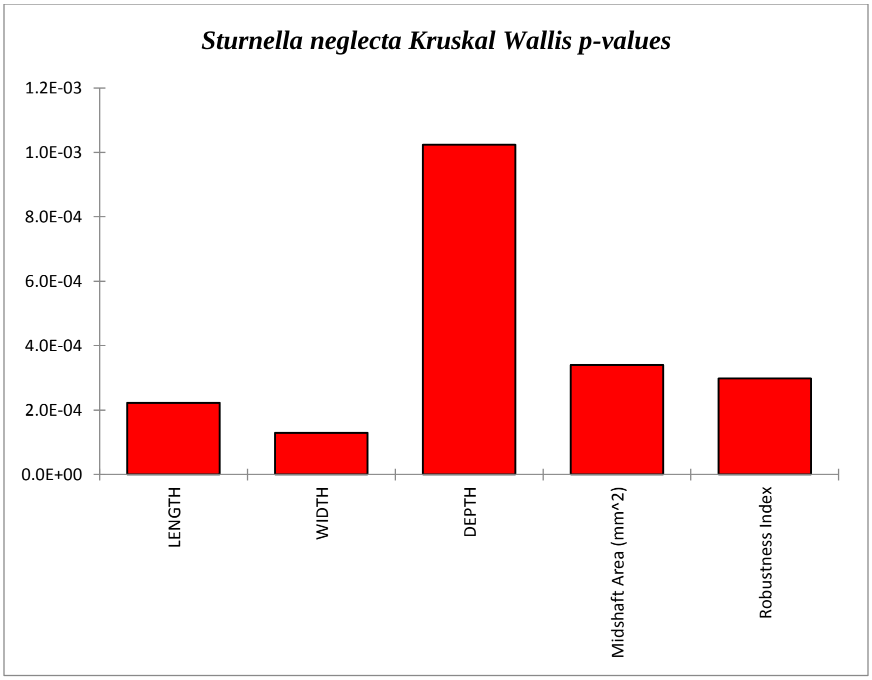

Figure 15. *Kruskal-Wallis p-values for Western Meadowlark including modern sample (above) and excluding modern sample (below). P-values less than 0.05 indicate significance in all TMT parameters in modern sample.*

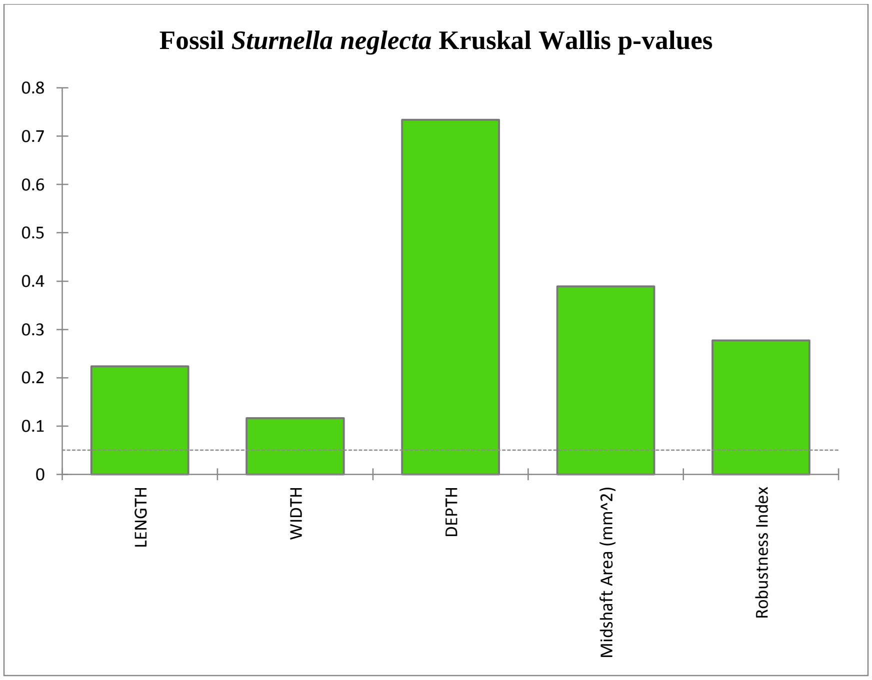

Results for *Sturnella neglecta* are important for this study, as this species is most comparable to species who have been reported with significant climate responses in body size. Contrast to expectations for this study, *Sturnella neglecta* actually change most significantly in the same manner as *Pica nutalli,* late morphological transition after the Pleistocene. These results further indicate conflict in gradualist models. With this final species results, I report stasis in all investigated species at La Brea through the Pleistocene.

Figure 16. *Western Meadowlark observations per parameter measured. Horizontal axis represents age in ka. Lines transect sample means. Kruskal-Wallis significance detected sample deviations in modern Sturnella neglecta for all TMT parameters; length, width, depth, midshaft area, and robustness index.*

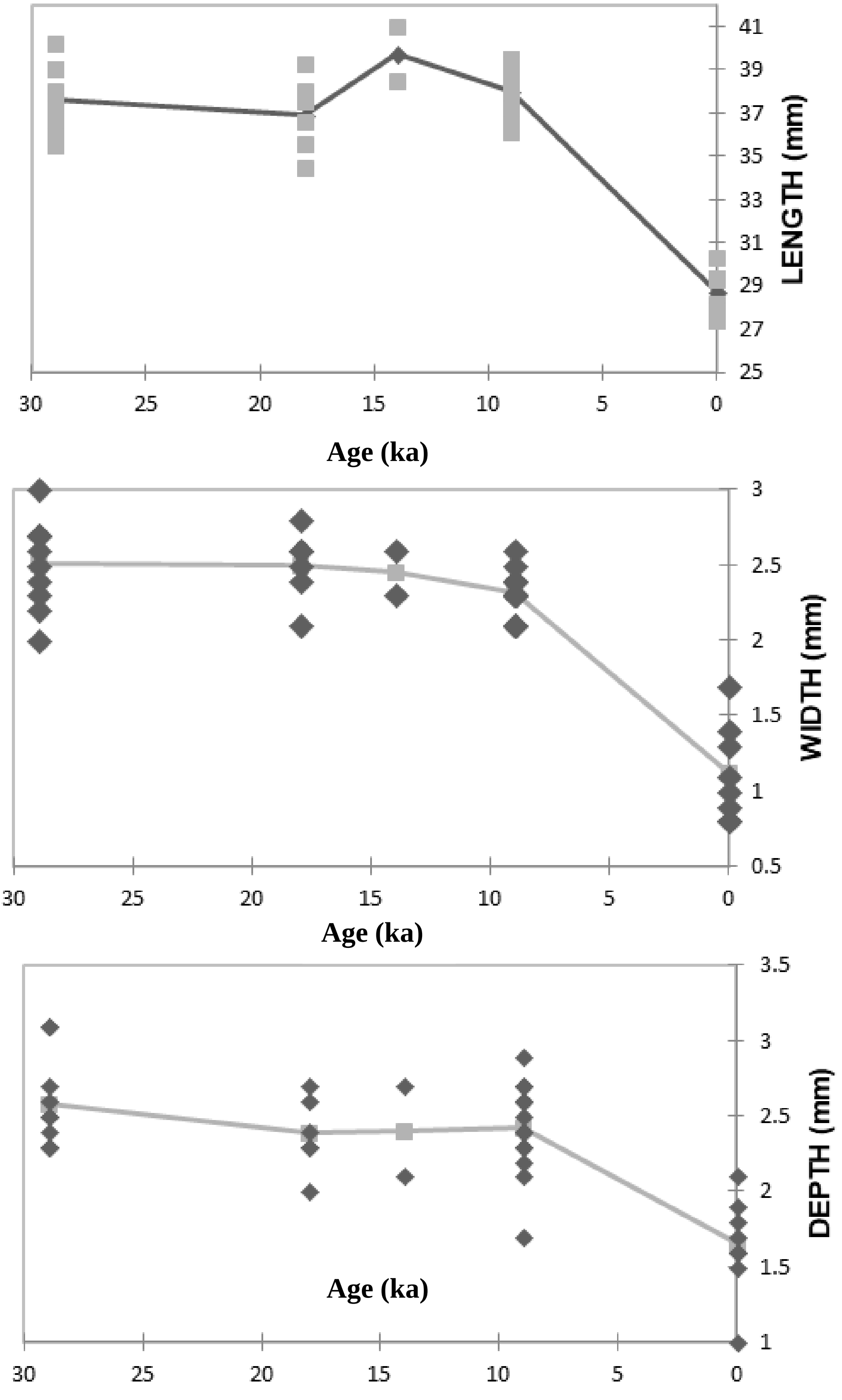

Figure 16. *Continued*

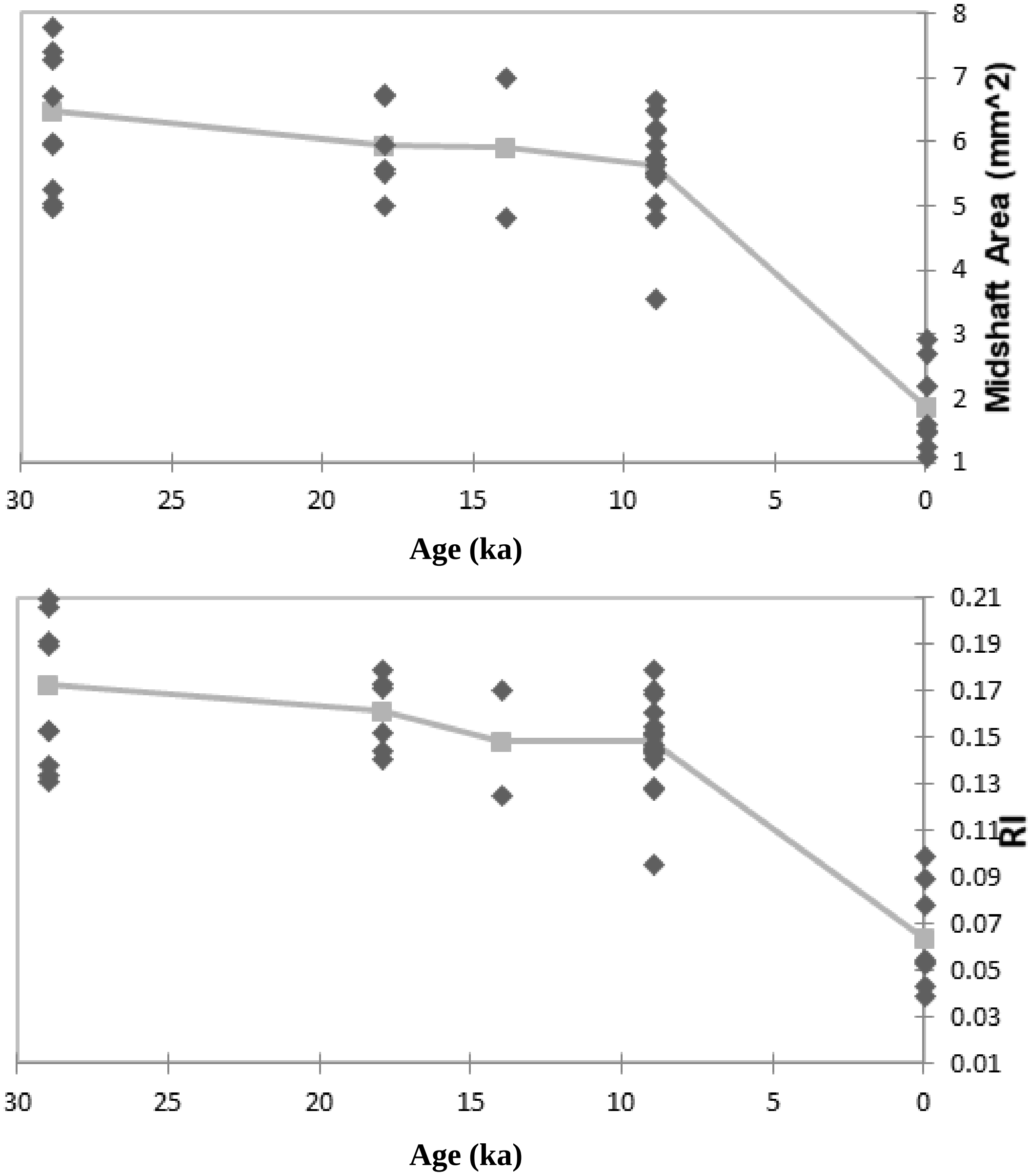

CHAPTER 4 – CONCLUSION

My research fails to support the effects of evolutionary generalizations of Bergman's and Allen's rule in investigated species during the RLB Pleistocene record. What changes we do see are mostly between the Pleistocene and modern species, not within the Pleistocene, and contrast those expected from the gradual change in species in response to climate change. It's clear that during the Pleistocene, climate cycles might have produced selection on species, and in some cases may have triggered their extinction. The climate however, is not seen to drive adaptive responses in principle morphologic features of body size and limb robustness. It would be appropriate to say that fossil small birds behaved in the same manner as other larger-bodied fossil species, with prolonged periods of morphological stasis, punctuated with short bursts of rapid change. To conclude, the phenomena of punctuated equilibrium is supported in RLB birds through my analysis.

4.1 – IMPLICATIONS OF MEGAFAUNAL EXTINCTION ON MODERN ASSEMBLAGES

The disappearance of many terrestrial mammals in the late Pleistocene likely influenced avifaunal diversity, perhaps most directly towards scavenging species like the vulture. Due to the vulture's obligatory carnivorous/scavenging diet, the dependence of terrestrial food sources may have been a factor in its demise, as the species did not survive past the Pleistocene-Holocene boundary (Fox-Dobbs, 2006). Furthermore, megafaunal disappearance wiped out niches in the La Brea ecosystem that very well affected the overall complexity of the habitat, an important environmental stressor. For example, the absence of large predators may have allowed prey animals to graze in areas that otherwise would have been avoided, cutting down vegetation that likely housed the habitat needed for other animals, such as *Sturnella n.* in this study. The lack of grass habitats would displace small predators who depended on prey animals living in those habitats, like raptors previously studied. These are just some examples of environmental stressors on RLB species correlated to megafaunal disappearances, that may have led to the changes seen against modern specimens in my study.

4.2 – CONCLUSION

Studies of clades of small-bodied birds, like the finches, have provided insights into the role of natural selection as a diversifying force, but cannot illuminate the processes that shape the diversity and discontinuities of radiations over longer evolutionary time frames (Leyequién, 2007). The models of bird evolution as exemplified through Darwin’s finches have proven to be less relevant to the larger-scale evolutionary patterns of birds than previously thought. Avian species are physically less variable than reptiles and mammals (Leyequién, 2007; Proctor, pg 13), making the argument that the group is already in an adaptive state, often living in a varied habitat. This explains a lack of expected variations in bird body plans at La Brea over the Pleistocene climatic cycles, which caused dramatic changes in the environment. Although this may be the case, it doesn’t explain the stasis of the non-bird species already described in the locality.

4.3 – FUTURE WORK

An assumption of the Kruskal Wallace test is that the distributions for the distinct groups to all be roughly the same other than changes in the median. The assumption in this data set can be debated, warranting the use of other and more advanced statistical analysis.

The comparison of TMT and wing proportions should be investigated, as the use of TMTs are often not used as a parameter in modern studies. Modern studies typically use wings as a parameter for body size, and since fossil wing elements are rarely preserved, they cannot be used in fossil studies. As such, an investigation of their relationship is reasonable.

REFERENCES

Akersten, W.A., Shaw, C.A. and Jefferson, G.T., 1983, Rancho La Brea: status and future: Paleobiology, v. 9, p. 211-217.

Brusatte, O'Connor, and Jarvis. (2015). The Origin and Diversification of Birds. Current Biology, 25(19), R888-R898.

Coltrain, J.B., Harris, J.M., Cerling, T.E., Ehleringer, J.R., Dearing, M., Ward, J., and Allen, J., 2004, Rancho La Brea stable isotope biogeochemistry and its implications for the palaeoecology of the late Pleistocene, coastal southern California: Palaeogeography, Palaeoclimatology, Palaeoecology , v. 205, p. 199-219.

Davis, B.L., 1997, A Field Guide to Birds of the Desert Southwest: Gulf Publishing Company, Houston, Texas.

DeSantis, S.N., Prothero, D.R., and Gage, G.L., 2011, Size and shape stasis in late Pleistocene horses and camels from Rancho La Brea during the last glacial-interglacial cycle: New Mexico Museum of Natural History Bulletin, v. 53, p. 505-510.

Eldredge, N., 1999, The Pattern of Evolution: W. H. Freeman, New York.

Eldredge, N., and Gould, S.J. 1972, Punctuated equilibria: An alternative to phyletic gradualism, p. 82-115, *in* Schopf, T.J.M. (ed.), Models in Paleobiology: Freeman, San Francisco,

Fragomeni, A., and Prothero, D.R., 2011, Stasis in late Quaternary birds from the La Brea tar pits during the last glacial-interglacial cycle: New Mexico Museum of Natural History Bulletin, v. 53, p. 511-516.

Fox-Dobbs, K., Stidman, T. A., Bowen, G. J., Emslie, S. D., & Koch, P. L., 2006, Dietary controls on extinction versus survival among avian megafauna in the late Pleistocene. Geology, v. 34, p. 685-688

Gardner, J., Amano, T., Backwell, P., Ikin, K., Sutherland, W., & Peters, A., 2014 Temporal patterns of avian body size reflect linear size responses to broadscale environmental change over the last 50 years. *Journal of Avian Biology, v.45, p. 525-535*

Gardner, J., Heinsohn, R., & Joseph, L., 2009, Shifting Latitudinal Clines in Avian Body Size Correlate with Global Warming in Australian Passerines. *Proceedings: Biological Sciences, vol. 276*, No.1674, p. 3845-3852.

Gould, S.J., 2002, The Structure of Evolutionary Theory: Harvard University Press, Cambridge, Massachusetts.

Grant, P.R. and Weiner, J., 1999, The Ecology and Evolution of Darwin's Finches: Princeton University Press, Princeton.

Grant, P.R. and Grant, B.R., 2007, How and Why Species Multiply: The Radiation of Darwin's Finches: Princeton University Press, Princeton.

Heusser, L., 1998, Direct correlation of millennial- scale changes in western North American vegetation and climate with changes in the California Current System over the past ~60 kyr, Paleoceanography, v. 13, p. 252–262.

Howard, H., 1949, A preliminary survey of trends in avian evolution from Pleistocene to recent time: The Condor, v. 49, p. 10-13.

Howard, H., 1962, A comparison of avian assemblages from individual pits at Rancho La Brea, California: Contributions in Science, Natural History Museum of Los Angeles County, v. 58, p. 1-24.

Kruskal, William H., & Wallis, W. Allen., 1952, Use of Ranks in One-Criterion Variance Analysis. *Journal of the American Statistical Association,* v. *47, No. 260, p. 583-621*

Leyequién, E., Boer, W., & Cleef, F., 2007 Influence of body size on coexistence of bird species. *Ecological Research,* v. *22,* p. 735-741

Lieberman, B.S. and Dudgeon, S., 1996, An evaluation of stabilizing selection as a mechanism for stasis: Palaeogeography, Palaeoclimatology, Palaeoecology, v. 127, p. 229-238

Madan, M., Prothero, D.R., and Sutyagina, A., 2011, Did felids from Rancho La Brea change size or shape in the last Pleistocene? New Mexico Museum of Natural History Bulletin, v. 53, p. 554-563

Madan, M., Prothero, R.D., and Syverson, J.V., 2015, Stasis in the Great Horned Owls from the La Brea Tar Pits during the last Glacial-Interglacial cycle: New Mexico Museum of Natural History and Science Bulletin v. 67, p. 221-226.

Madan, M., D.R. Prothero, and V.J.P. Syverson, 2016. Stasis in barn owls from the La Brea tar pits during the last glacial-interglacial cycle. *New Mexico Museum of Natural History Bulletin* 74: 153-157.

Marcus, L.F. and Berger, R., 1984, The significance of radiocarbon dates for Rancho La Brea, p. 159-188, *in* Martin, P.S. and Klein, R.G. (eds.), Quaternary Extinctions: A Prehistoric Revolution: University of Chicago Press, Chicago.

Mason, N., & Burns, K. (2015). The effect of habitat and body size on the evolution of vocal displays in Thraupidae (tanagers), the largest family of songbirds. *Biological Journal of the Linnean Society, 114*(3), 538-551

Meiri, S., and Dayan T., 2003, On the Validity of Bergmann's Rule: Journal of Biogeography. v. 30(3), p. 331-351.

Molina, S., and Prothero, D.R., 2011, Evolutionary stasis in late Pleistocene golden eagles: New Mexico Museum of Natural History Bulletin, v. 53, p. 64-569.

O’Keefe, F.R., Fet, E.V., and Harris, J.M., 2009, Compilation, calibration, and synthesis of faunal and floral radiocarbon dates, Rancho la Brea, California: Contributions in Science, Natural History Museum of Los Angeles County, v. 518, p. 1-16.

Proctor, N.S. and Lynch, P.J., 1993, Manual of Ornithology: Yale University, New Haven and London.

Prothero, D.R., and Raymond, K.R., 2008, Variability and sexual size dimorphism in Pleistocene ground sloths (Xenarthra): New Mexico Museum of Natural History and Science Bulletin, v. 44, p. 331-334.

Prothero, D.R., and Raymond, K.R., 2011, Stasis in late Pleistocene ground sloths (*Paramylodon harlani*) from Rancho La Brea, California: New Mexico Museum of Natural History Bulletin, v. 53, p. 624-628.

Sibley, D.A., 2003, The Sibley Field Guide to Birds of Western North America: Alfred A. Knopf, New York.

Symonds, MRE, and GJ Tattersall, 2010, Geographical Variation in Bill Size Across Bird Species Provides Evidence for Allen's Rule: American Naturalist, v. 176(2), p. 188-197.

Syverson, V.J., and Prothero, D.R., 2010, Evolutionary patterns in late Quaternary California condors: PalArch Journal of Vertebrate Paleontology, v. 7(10), p. 1-18.

Weiner, J., 1995, The Beak of the Finch: A Story of Evolution in our Own Time: Vintage. New York.

Weiner, J., 1995, Evolution Made Visible: Science. v. 267(5194), p. 30-33.

Zink, R., 2002, A New Perspective on the Evolutionary History of Darwin's Finches: The Auk, v. 119(3), p. 864-871.

APPENDIX A: DATA

Table A. 1 *Coragyps occidentalis* TMT data from collections at Rancho La Brea Tar Pits

CAT. #	PIT	Age (ka)	LENGTH (mm)	WIDTH (mm)	DEPTH (mm)	Midshaft Area (mm^2)	Robustness Index (Midshaft Area/Length)
D8142	4	14	59.2	7.2	6	43.2	0.72972973
D88142	4	14	57.1	7.4	6	44.4	0.777583187
D7327	4	14	55	7.9	5.4	42.66	0.775636364
D7389	4	14	56	7.9	5.5	43.45	0.775892857
D8283	4	14	52.6	8.2	6	49.2	0.935361217
D7070	4	14	57.2	8.4	5.7	47.88	0.837062937
D8280	4	14	60	6.9	5.7	39.33	0.6555
D7287	4	14	57.8	6.9	5.7	39.33	0.680449827
D7289	4	14	58.2	9	6.6	59.4	1.020618557
D8321	4	14	58.8	8.3	6.4	53.12	0.903401361
D7769	4	14	54.1	7.2	6.1	43.92	0.811829945
D7016	4	14	57.4	8.1	6.5	52.65	0.917247387
D7430	4	14	57.7	7.8	6.1	47.58	0.824610052
D8086	4	14	57.2	8	5.6	44.8	0.783216783
D7266	4	14	60.8	7	5.9	41.3	0.679276316
D7385	4	14	57.2	6.8	5.6	38.08	0.665734266
D7838	4	14	60.8	6.6	5.9	38.94	0.640460526
D7778	4	14	59.7	7.6	6.3	47.88	0.80201005
D7651	4	14	58	6.8	5.3	36.04	0.62137931
D7047	4	14	58	7	6.5	45.5	0.784482759
D8361	4	14	61.1	7.2	5.6	40.32	0.6599018
D7429	4	14	59.2	8.8	6	52.8	0.891891892
D8464	4	14	59.2	7.8	6	46.8	0.790540541
D7456	4	14	56.1	6.3	5.6	35.28	0.628877005
D7135	4	14	57.1	8.1	5.6	45.36	0.794395797
D7146	4	14	55.3	7.4	6	44.4	0.802893309
D7849	4	14	56.3	7.9	6.4	50.56	0.898046181
D7989	4	14	56.3	7.5	5.9	44.25	0.785968028
D7048	4	14	58.7	7.2	5	36	0.613287905
D8193	4	14	50.7	6.6	6.1	40.26	0.79408284
D7162	4	14	52.7	6.9	6	41.4	0.785578748
D7045	4	14	54	6.8	5.2	35.36	0.654814815
D7231	4	14	53.2	7.7	5.3	40.81	0.767105263

Table A. 1. (Continued)

CAT. #	PIT	Age (ka)	LENGTH (mm)	WIDTH (mm)	DEPTH (mm)	Midshaft Area (mm^2)	Robustness Index (Midshaft Area/Length)
D7273	4	14	57.8	6.5	4.7	30.55	0.528546713
D8008	4	14	58.8	6.8	5.3	36.04	0.61292517
D7169	4	14	61.1	7.6	5.4	41.04	0.671685761
D7419	4	14	58.8	6.7	5.7	38.19	0.649489796
D7993	4	14	54.5	7	5.4	37.8	0.693577982
D7465	4	14	53.8	7	4.9	34.3	0.637546468
D7884	4	14	54.6	7.9	5.6	44.24	0.81025641
D7306	4	14	57.8	7.3	5.6	40.88	0.707266436
D7194	4	14	60.1	6.6	4.9	32.34	0.538103161
D7416	4	14	61	7.6	5.9	44.84	0.735081967
D8160	4	14	59.4	8.4	5.9	49.56	0.834343434
D7211	4	14	56.2	7.4	5.2	38.48	0.684697509
D8316	4	14	57.8	7.7	4.7	36.19	0.626124567
D8007	4	14	58.7	6.7	4.6	30.82	0.525042589
D8469	4	14	58.6	7	5.6	39.2	0.66894198
D8179	4	14	55.9	8.4	5.9	49.56	0.886583184
D7834	4	14	56.2	7.5	5.3	39.75	0.707295374
D7198	4	14	57.3	7	5	35	0.610820244
D7212	4	14	54.1	8	5.4	43.2	0.798521257
D7575	4	14	56	7.6	6	45.6	0.814285714
D8407	4	14	55.2	7.4	5.5	40.7	0.737318841
D8884	3	18	54.2	7.5	6	45	0.830258303
D8952	3	18	55.9	8	6	48	0.858676208
D8724	3	18	55.1	7.7	6.3	48.51	0.880399274
D8779	3	18	57.3	8.1	6.1	49.41	0.862303665
D9048	3	18	51.4	8	6.3	50.4	0.980544747
D8907	3	18	59.1	8.6	5.6	48.16	0.814890017
D9141	3	18	54.7	7.7	6.2	47.74	0.872760512
D8942	3	18	55.7	8.8	6	52.8	0.947935368
D8794	3	18	57.6	7.8	5.9	46.02	0.798958333
D8959	3	18	58.8	9	6.5	58.5	0.994897959
D8515	3	18	56.8	6.8	6.2	42.16	0.742253521
D9122	3	18	52.3	6.8	5.5	37.4	0.715105163
D8902	3	18	66.9	8.1	6.3	51.03	0.762780269
D8840	3	18	57.6	8.3	5.1	42.33	0.734895833
D8567	3	18	60	7.6	5.3	40.28	0.671333333
D8501	3	18	57.8	8	6.1	48.8	0.844290657
D9157	3	18	56.2	7.4	5.7	42.18	0.750533808

Table A. 1. (Continued)

CAT. #	PIT	Age (ka)	LENGTH (mm)	WIDTH (mm)	DEPTH (mm)	Midshaft Area (mm^2)	Robustness Index (Midshaft Area/Length)
D9154	3	18	57.9	7.3	5.8	42.34	0.731260794
D9084	3	18	52.3	7.2	6.3	45.36	0.867304015
D9075	3	18	50.8	7.4	5.2	38.48	0.757480315
D9095	3	18	51.8	8	6.2	49.6	0.957528958
D8848	3	18	54.3	7.6	5.4	41.04	0.755801105
D8572	3	18	55.6	7.4	5.8	42.92	0.771942446
D8587	3	18	64.8	7.4	5.9	43.66	0.673765432
D8493	3	18	52.3	7.6	5.7	43.32	0.828298279
D8564	3	18	57.9	6.9	5.5	37.95	0.655440415
D8546	3	18	55.4	7.3	5.1	37.23	0.672021661
D8791	3	18	54.3	7.2	5.4	38.88	0.716022099
D9158	3	18	54.1	7.2	5.1	36.72	0.678743068
D8644	3	18	58.1	7.4	5.6	41.44	0.713253012
D9130	3	18	54.8	7.2	4.7	33.84	0.617518248
D8710	3	18	54.3	7.4	4.7	34.78	0.640515654
D9027	3	18	56.2	6.5	5.1	33.15	0.589857651
D9113	3	18	57.6	6.6	5.6	36.96	0.641666667
D8980	3	18	56.9	7.8	5.7	44.46	0.781370826
D8705	3	18	58	7.5	5	37.5	0.646551724
D8768	3	18	58.9	7.4	5.8	42.92	0.728692699
D8625	3	18	55.7	7.4	5.3	39.22	0.704129264
D8670	3	18	59.3	7.3	6.1	44.53	0.750927487
D8618	3	18	57.3	7.6	5.3	40.28	0.702966841
D8742	3	18	55.4	7	5.4	37.8	0.682310469
D8846	3	18	56.6	6.8	5.3	36.04	0.636749117
D8573	3	18	53	7.6	5.6	42.56	0.803018868
D9036	3	18	57	7.4	5.5	40.7	0.714035088
D8975	3	18	59.8	8.3	5.7	47.31	0.791137124
D9020	3	18	59.5	8	5.8	46.4	0.779831933
D8559	3	18	56.9	8.1	5.8	46.98	0.825659051
D8999	3	18	55.1	6.6	5	33	0.598911071
D9163	3	18	56.4	6.5	4.9	31.85	0.564716312
D8545	3	18	58.3	7.9	6	47.4	0.813036021
D8859	3	18	52.7	7.9	5.6	44.24	0.839468691
D8939	3	18	50.1	6.9	5	34.5	0.688622754
D9171	3	18	57.9	8	5.8	46.4	0.801381693

Table A. 1. (Continued)

CAT. #	PIT	Age (ka)	LENGTH (mm)	WIDTH (mm)	DEPTH (mm)	Midshaft Area (mm^2)	Robustness Index (Midshaft Area/Length)
D8524	3	18	54.3	7.1	5.1	36.21	0.666850829
D8833	3	18	57.2	8.1	5.6	45.36	0.793006993
D8771	3	18	57.3	7.3	5.5	40.15	0.70069808
D8574	3	18	54	7.5	5.1	38.25	0.708333333
D8888	3	18	54.6	6.4	5.2	33.28	0.60952381
D8718	3	18	57.7	7.3	5.7	41.61	0.721143847
D8570	3	18	60	7.4	5.9	43.66	0.727666667
D9837	60	21	57.3	8.3	6.2	51.46	0.898080279
D9845	60	21	57.1	7.7	6.1	46.97	0.822591944
D9874	60	21	56.8	6.4	6	38.4	0.676056338
D9880	60	21	56.2	7.9	5.7	45.03	0.801245552
D9895	60	21	58.5	6.9	5.6	38.64	0.660512821
D9855	60	21	55.5	7.1	5.7	40.47	0.729189189
D9876	60	21	57	7.3	5	36.5	0.640350877
D9836	60	21	57.8	7.2	5.3	38.16	0.660207612
D9832	60	21	57.9	6.9	5.1	35.19	0.607772021
D9872	60	21	59.3	7.6	5.5	41.8	0.704890388
D9828	60	21	58	6.8	5.1	34.68	0.597931034
D9877	60	21	55.8	7	5.9	41.3	0.740143369
D9887	60	21	58.7	7.9	5.8	45.82	0.780579216
D9939	77	35	58.6	9	6.8	61.2	1.044368601
D9954	77	35	52.3	8	5.5	44	0.841300191
D9982	77	35	55.6	7	5	35	0.629496403
D9938	77	35	56.5	6.8	5.5	37.4	0.661946903
D9993	77	35	55.5	7.6	5.4	41.04	0.739459459
D9966	77	35	55	8.1	5.7	46.17	0.839454545
D9967	77	35	59.5	7.9	5.3	41.87	0.703697479
D9952	77	35	57.3	7.6	6	45.6	0.795811518
D9918	77	35	55.6	7.2	5.8	41.76	0.751079137

Table A. 2. Collected *Coragyps atratus* TMT data from University of Vertebrate Zoology and American Museum. Diaphysis length calculated in American Museum specimens.

Age (ka)	LENGTH (mm)	WIDTH (mm)	DEPTH (mm)	Midshaft Area (mm^2)	Robustness Index
0	51.44444444	9.2	7	64.4	1.251835853
0	58.0096	9.2	7.4	68.08	1.173598853
0	59.9104	8	7	56	0.934729196
0	59.9808	9.4	7.5	70.5	1.17537612
0	60.192	8.7	6	52.2	0.86722488
0	59.84	7.4	5.2	38.48	0.643048128
0	58.432	8.3	6	49.8	0.852272727
0	58.08	7.8	6.5	50.7	0.872933884
0	61.4592	6.7	6	40.2	0.654092471
0	59.84	7.5	6.8	51	0.852272727
0	60.896	7.8	6.7	52.26	0.858184446
0	60.544	8.2	6.5	53.3	0.88035148
0	62.656	7.6	6.8	51.68	0.824821246
0	60.544	7	6	42	0.693710359
0	60.544	6.1	5.7	34.77	0.574293076
0	60.2624	7.8	6.3	49.14	0.815433836
0	59.9808	8	6.3	50.4	0.840268886
0	57.024	7.7	6	46.2	0.810185185
0	57.024	7.5	6	45	0.789141414
0	59.136	8	7.3	58.4	0.987554113
0	58.0096	8.3	6.7	55.61	0.958634433
0	58.432	7.5	6.1	45.75	0.782961391
0	55.264	9.6	6.1	58.56	1.059640996
0	56.9536	8.5	6	51	0.895465783
0	59.488	7.5	6	45	0.756455083
0	59.3472	7.1	6.2	44.02	0.741736763
0	59.488	7.7	6.7	51.59	0.867233728
0	59.6288	7.5	6	45	0.754668885
0	58.7	6.8	5.6	38.08	0.648722317
0	59.1	6.5	5.4	35.1	0.593908629
0	58.4	6.3	5.2	32.76	0.560958904
0	58.2	6.6	5.2	34.32	0.589690722
0	56.7	6.1	4.8	29.28	0.516402116
0	56.2	6.2	4.4	27.28	0.485409253
0	58.1	6.2	4.9	30.38	0.522891566
0	57.6	6	4.8	28.8	0.5

Table A. 3. Collected *Corvus corax* TMT data from collections at Rancho La Brea Tar Pits

PIT	Age (ka)	LENGTH (mm)	WIDTH (mm)	DEPTH (mm)	Midshaft Area (mm^2)	Robustness Index
10	9	44.4	5.3	4.6	24.38	0.549099099
10	9	48.7	5.3	4	21.2	0.435318275
10	9	46	4.2	3.6	15.12	0.328695652
10	9	46.8	4.4	4.3	18.92	0.404273504
10	9	42.6	4.4	4.2	18.48	0.433802817
10	9	44	4.4	3.5	15.4	0.35
10	9	40.3	3.8	3.5	13.3	0.330024814
10	9	48	4.6	4.4	20.24	0.421666667
10	9	46.1	3.1	4.1	12.71	0.275704989
10	9	48.3	4.3	4	17.2	0.35610766
10	9	52.2	5	4.8	24	0.459770115
10	9	48.4	4.7	4.2	19.74	0.40785124
10	9	45.7	4.2	5	21	0.4595186
10	9	45.6	4.2	4.2	17.64	0.386842105
10	9	44.2	4.7	5.2	24.44	0.552941176
10	9	46.1	3.7	4.1	15.17	0.329067245
10	9	47.5	3.6	4.5	16.2	0.341052632
10	9	47.2	4	3.6	14.4	0.305084746
10	9	40.6	3.8	4.7	17.86	0.439901478
10	9	43.6	4.1	4	16.4	0.376146789
10	9	42.2	4.5	4	18	0.426540284
10	9	44.2	4	4.5	18	0.407239819
10	9	42.1	4.8	4.3	20.64	0.490261283
10	9	45	4.2	4.8	20.16	0.448
10	9	42.8	3.7	4.5	16.65	0.389018692
10	9	42.6	3.5	3.1	10.85	0.254694836
10	9	41.2	4.5	3.3	14.85	0.360436893
10	9	46.5	4.7	4.5	21.15	0.45483871
10	9	44.3	4.3	3.9	16.77	0.378555305
10	9	47.5	3.6	4.1	14.76	0.310736842
10	9	44.7	4	4.8	19.2	0.429530201
10	9	49.5	4.1	5.9	24.19	0.488686869
10	9	48.5	4.5	4.8	21.6	0.445360825
10	9	44.3	3.9	4.3	16.77	0.378555305
10	9	45.9	4	3.9	15.6	0.339869281
10	9	45.8	3.6	3.5	12.6	0.27510917
10	9	41.9	3.7	3.8	14.06	0.335560859

Table A. 3. (Continued)

PIT	Age (ka)	LENGTH (mm)	WIDTH (mm)	DEPTH (mm)	Midshaft Area (mm^2)	Robustness Index
10	9	48.4	4.3	4.6	19.78	0.408677686
10	9	49.2	3.9	5.3	20.67	0.420121951
10	9	48.6	4.8	4.9	23.52	0.483950617
10	9	44	3.9	4.4	17.16	0.39
10	9	49.2	4.2	4.1	17.22	0.35
10	9	48.4	4.3	5	21.5	0.444214876
10	9	46	4.3	4.1	17.63	0.38326087
10	9	44	4.5	4.7	21.15	0.480681818
10	9	45.7	4	3.9	15.6	0.341356674
10	9	46.7	4.5	4.5	20.25	0.433618844
10	9	46.5	4.1	4.5	18.45	0.396774194
10	9	49.1	4	3.8	15.2	0.309572301
10	9	42.8	4	4.3	17.2	0.401869159
10	9	45.7	3.7	4.5	16.65	0.364332604
10	9	47	4.5	4.1	18.45	0.392553191
10	9	48	4.1	5.3	21.73	0.452708333
10	9	48	4.6	4.4	20.24	0.421666667
10	9	49.1	4.9	4.8	23.52	0.479022403
10	9	47.4	4.5	4.3	19.35	0.408227848
10	9	47.3	4.3	4.5	19.35	0.409090909
10	9	41.8	4	4.5	18	0.43062201
10	9	47.4	4.2	4.6	19.32	0.407594937
10	9	46	3.7	4.1	15.17	0.329782609
10	9	46.7	4.1	3.6	14.76	0.316059957
10	9	50.6	5.7	5.5	31.35	0.619565217
10	9	46.2	3.3	4.2	13.86	0.3
10	9	49.2	4.3	4.4	18.92	0.384552846
10	9	44.8	4.3	3.8	16.34	0.364732143
10	9	46.7	4	4.6	18.4	0.394004283
10	9	46	3.9	4.3	16.77	0.364565217
10	9	46.6	4.3	5	21.5	0.461373391
10	9	46.6	3.2	4.1	13.12	0.281545064
10	9	48.2	5	4.2	21	0.435684647
10	9	49.7	4.8	4.6	22.08	0.444265594
10	9	48.7	4.4	5.1	22.44	0.460780287
10	9	44.3	4.3	4.2	18.06	0.407674944
10	9	47.3	4.3	3.9	16.77	0.354545455
10	9	47.2	3.7	3.3	12.21	0.258686441

Table A. 3. (Continued)

PIT	Age (ka)	LENGTH (mm)	WIDTH (mm)	DEPTH (mm)	Midshaft Area (mm^2)	Robustness Index
10	9	42.1	3.6	3.9	14.04	0.333491686
10	9	44.5	4.5	3.7	16.65	0.374157303
10	9	44	4.2	3.4	14.28	0.324545455
10	9	47.6	4.2	3.6	15.12	0.317647059
10	9	48.4	3.9	4.5	17.55	0.362603306
10	9	46.9	4.2	4.2	17.64	0.376119403
61	11	46.3	4.2	3.3	13.86	0.299352052
61	11	48	3.9	4.3	16.77	0.349375
61	11	49.4	4.2	4.6	19.32	0.391093117
61	11	42.5	3.9	4.1	15.99	0.376235294
61	11	47.2	5.5	4.3	23.65	0.501059322
61	11	44.2	4	3.8	15.2	0.343891403
61	11	45.1	3.7	4.4	16.28	0.36097561
4	14	42.8	4.3	5	21.5	0.502336449
4	14	44.2	4	4.7	18.8	0.425339367
4	14	49.5	5.7	4.8	27.36	0.552727273
4	14	47.2	4	4.8	19.2	0.406779661
4	14	47.5	4.5	4.4	19.8	0.416842105
4	14	43.5	4.2	4.3	18.06	0.415172414
4	14	45.6	3.8	4.6	17.48	0.383333333
4	14	42	3.8	4.3	16.34	0.389047619
4	14	49	4.1	5	20.5	0.418367347
4	14	45.8	4.8	3.7	17.76	0.387772926
4	14	46	4.2	4.8	20.16	0.43826087
4	14	43.2	4	4.5	18	0.416666667
4	14	42.6	3.7	4.5	16.65	0.39084507
4	14	45.2	4	5.3	21.2	0.469026549
4	14	45.8	3.7	4.8	17.76	0.387772926
4	14	46.9	3.6	3.8	13.68	0.291684435
4	14	46.6	4.1	5.1	20.91	0.448712446
4	14	44.3	3.6	4.5	16.2	0.365688488
4	14	45.2	3.9	5	19.5	0.431415929
4	14	44.3	4.3	5	21.5	0.485327314
4	14	42.9	3.7	4.9	18.13	0.422610723
4	14	45.7	4.3	5.7	24.51	0.536323851
4	14	45.8	3.9	5.1	19.89	0.434279476
4	14	50.8	3.6	4.9	17.64	0.347244094
4	14	49	4.1	4.5	18.45	0.376530612

Table A.3. (Continued)

PIT	Age (ka)	LENGTH (mm)	WIDTH (mm)	DEPTH (mm)	Midshaft Area (mm^2)	Robustness Index
4	14	46.7	3.7	4.9	18.13	0.388222698
4	14	48.5	4.1	3.9	15.99	0.329690722
4	14	44.5	4	4.5	18	0.404494382
4	14	49	4.2	5.2	21.84	0.445714286
4	14	45.2	4.2	3.3	13.86	0.306637168
4	14	47.5	4	5	20	0.421052632
4	14	44.7	4.3	4.5	19.35	0.432885906
13	16	41.8	4.4	3.5	15.4	0.368421053
13	16	49.3	4.8	5.7	27.36	0.554969574
13	16	47.3	3.9	4.4	17.16	0.362790698
13	16	50.2	3.9	5.4	21.06	0.419521912
13	16	46.2	5.9	4.8	28.32	0.612987013
13	16	41.9	4.1	5.4	22.14	0.528400955
3	18	44.4	4.1	4.7	19.27	0.434009009
3	18	51	5	5.5	27.5	0.539215686
3	18	45.6	4.3	5	21.5	0.471491228
3	18	45.7	4	4.3	17.2	0.376367615
3	18	49.3	3.5	3.8	13.3	0.269776876
3	18	46	3.6	3.4	12.24	0.266086957
3	18	45.6	4.2	5.1	21.42	0.469736842
3	18	46.7	3.7	4.8	17.76	0.380299786
3	18	47	4.1	4.4	18.04	0.383829787
3	18	47.2	3.5	4.7	16.45	0.348516949
3	18	47.5	3.8	4	15.2	0.32
3	18	43.6	3.7	5	18.5	0.424311927
3	18	43.7	4.5	4.4	19.8	0.453089245
3	18	44.7	4.3	4.7	20.21	0.45212528
60	21	49	4	4.9	19.6	0.4
	29	39.6	3.8	4.5	17.1	0.431818182
	29	39.9	3.9	3.2	12.48	0.312781955
	29	42.6	4.2	4	16.8	0.394366197
	29	42	3.6	4.5	16.2	0.385714286
	29	44.6	4.2	4.3	18.06	0.404932735
	29	47.7	4	4.7	18.8	0.394129979
	29	45	3.7	4.6	17.02	0.378222222
	29	46.7	3.8	4.3	16.34	0.349892934
	29	58.3	4.6	4.7	21.62	0.37084048

Table A. 4. Collected *Corvus corax* TMT data from University of Vertebrate Zoology and American Museum. Diaphysis length calculated in American Museum specimens.

Age (ka)	LENGTH (mm)	WIDTH (mm)	DEPTH (mm)	Midshaft Area (mm^2)	Robustness Index
0	44.3125	4.8	5.5	26.4	0.595768688
0	47.7125	5.5	5.9	32.45	0.680115274
0	48.3125	5.2	4.9	25.48	0.527399741
0	47.8125	5	6	30	0.62745098
0	47.4125	5.1	5	25.5	0.53783285
0	48.3125	5.1	5.1	26.01	0.538369987
0	47.3125	5.1	5.7	29.07	0.614425363
0	50	3.9	4.5	17.55	0.351
0	49.6	3.9	4.7	18.33	0.369556452
0	48.2	3.7	4.5	16.65	0.345435685
0	49.7	3.6	4.5	16.2	0.325955734
0	43.4	3.8	5.2	19.76	0.455299539
0	44.3	3.8	5.1	19.38	0.437471783
0	44.3	4	5.2	20.8	0.469525959
0	44.8	3.8	4.9	18.62	0.415625

Table A. 5 *Pica nutalli* TMT data from collections at Rancho La Brea Tar Pits

AGE (ka)	LENGTH (mm)	WIDTH (mm)	DEPTH (mm)	Midshaft Area (mm^2)	Robustness Index
9	45.8	2.5	2.5	6.25	0.136462882
9	45.2	2.1	2.5	5.25	0.116150442
11	46.4	2.6	3	7.8	0.168103448
11	47.1	2.5	3	7.5	0.159235669
14	46.5	2.4	2.6	6.24	0.134193548
14	48	2.9	2.4	6.96	0.145
14	47	2.5	2.8	7	0.14893617
14	41.8	2.7	2.5	6.75	0.161483254
14	46.6	2.3	2.8	6.44	0.138197425
14	47.4	2.2	3	6.6	0.139240506
14	45.3	2.8	3	8.4	0.185430464
14	47.5	2.6	2.8	7.28	0.153263158
14	45.5	2.3	2.5	5.75	0.126373626
14	46.7	2.5	3.6	9	0.192719486
14	48.1	2.3	2.9	6.67	0.138669439
16	46.8	3	2.8	8.4	0.179487179
16	47.1	3	2.5	7.5	0.159235669
16	49.3	2.5	2.7	6.75	0.136916836
18	47.8	2.4	3.1	7.44	0.155648536
18	47.5	2.4	2.8	6.72	0.141473684
29	43.2	3	2.8	8.4	0.194444444

Table A. 6. Collected *Pica nutalli* TMT data from University of Vertebrate Zoology and American Museum. Diaphysis length calculated in American Museum specimens.

AGE (ka)	LENGTH (mm)	WIDTH (mm)	DEPTH (mm)	Midshaft Area (mm^2)	Robustness Index
0	34.7	1.3	2	2.6	0.074927954
0	36.1	1.3	2.5	3.25	0.090027701
0	38.4	1.4	2.5	3.5	0.091145833
0	42.3	1.3	2.2	2.86	0.067612293
0	38.6	1.4	1.7	2.38	0.061658031
0	38.9	1.3	1.8	2.34	0.060154242
0	35	1.2	1.6	1.92	0.054857143
0	37.8	1.2	1.7	2.04	0.053968254
0	35.575	2.8	3.3	9.24	0.259732959
0	36.575	3	2.5	7.5	0.2050581
0	33.075	2.2	3.5	7.7	0.232804233
0	33.575	2.5	2.5	6.25	0.18615041
0	34.075	2.3	2.4	5.52	0.161995598

Table A.7. *Sturnella neglecta* TMT data from collections at Rancho La Brea Tar Pits

AGE	LENGTH	WIDTH	DEPTH	Midshaft Area (mm^2)	Robustness Index
9	36.3	2.4	2.3	5.52	0.152066116
9	37.5	2.3	2.1	4.83	0.1288
9	36.1	2.5	2.6	6.5	0.180055402
9	38	2.3	2.4	5.52	0.145263158
9	39.5	2.3	2.9	6.67	0.168860759
9	37.2	2.1	1.7	3.57	0.095967742
9	39	2.3	2.5	5.75	0.147435897
9	38	2.1	2.6	5.46	0.143684211
9	38.5	2.6	2.3	5.98	0.155324675
9	37.2	2.1	2.7	5.67	0.152419355
9	38.5	2.3	2.7	6.21	0.161298701
9	36.5	2.4	2.6	6.24	0.170958904
9	39	2.3	2.4	5.52	0.141538462
9	39.5	2.4	2.4	5.76	0.145822785
9	39.3	2.3	2.2	5.06	0.128753181
14	41	2.6	2.7	7.02	0.171219512
14	38.5	2.3	2.1	4.83	0.125454545
18	37.5	2.5	2.7	6.75	0.18
18	36.6	2.8	2	5.6	0.153005464
18	38	2.4	2.3	5.52	0.145263158
18	39.3	2.6	2.6	6.76	0.172010178
18	34.5	2.6	2.3	5.98	0.173333333
18	35.6	2.1	2.4	5.04	0.141573034
29	39	2.5	2.4	6	0.153846154
29	36.5	2.2	2.3	5.06	0.138630137
29	37.2	3	2.6	7.8	0.209677419
29	38	2.7	2.7	7.29	0.191842105
29	37.5	2.7	3.1	8.37	0.2232
29	35.5	2.7	2.5	6.75	0.190140845
29	37.2	2	2.5	5	0.134408602
29	39	2.6	2.3	5.98	0.153333333
29	36	2.4	3.1	7.44	0.206666667
29	40.2	2.3	2.3	5.29	0.13159204

APPENDIX B: MODERN DATA

Table B. 1. *Coragyps atratus* observational data from the Museum of Vertebrate Zoology

Museum of Vertebrate Zoology						
CAT. #	**Sex**	**Side**	**Diaphysis (mm)**	**Length (mm)**	**Width (mm)**	**Depth (mm)**
MVZBIRD79208	M	Right	58.7	85.6	6.8	5.6
MVZBIRD79208	M	Left	59.1	85.4	6.5	5.4
MVZBIRD79210	M	Right	58.4	80.4	6.3	5.2
MVZBIRD79210	M	Left	58.2	80.4	6.6	5.2
MVZBIRD79209	F	Right	56.7	81.8	6.1	4.8
MVZBIRD79209	F	Left	56.2	82.4	6.2	4.4
MVZBIRD78681	M	Right	58.1	81.2	6.2	4.9
MVZBIRD78681	M	Left	57.6	80.8	6	4.8

Table B. 2. *Coragyps atratus* observational data from American Museum of Natural History

American Museum of Natural History			
ID	**Length (mm)**	**Width (mm)**	**Depth (mm)**
Female1	83	9.2	7
Female1	82.4	9.2	7.4
Female2	85.1	8	7
Female2	85.2	9.4	7.5
Female3	85.5	8.7	6
Female3	85	7.4	5.2
Female4	83	8.3	6
Female4	82.5	7.8	6.5
Female5	87.3	6.7	6
Female5	85	7.5	6.8
Male6	86.5	7.8	6.7
Male6	86	8.2	6.5
Female7	89	7.6	6.8
Female7	86	7	6
Male8	86	6.1	5.7
Male9	85.6	7.8	6.3
Male9	85.2	8	6.3
Female10	81	7.7	6
Female10	81	7.5	6
Female11	84	8	7.3
Female12	82.4	8.3	6.7
Female12	83	7.5	6.1
Female13	78.5	9.6	6.1
Female13	80.9	8.5	6
Female14	84.5	7.5	6
Female14	84.3	7.1	6.2
Female15	84.5	7.7	6.7
Female15	84.7	7.5	6

Table B. 3. *Corvus corax* observational data from the Museum of Vertebrate Zoology. Two subspecies were noted, and a mean articular length was calculated for use of American Museum specimens.

Museum of Vertebrate Zoology									
Corvus corax sinuatus									
CAT. #	Sex	Side	Diaphysis	Length	Width	Depth	Diff.	Area	Robustness
MVZBIRD184170	-	Right	50	66.4	3.9	4.5	16.4	17.55	0.2643072
MVZBIRD184170	-	Left	49.6	67.1	3.9	4.7	17.5	18.33	0.2731743
MVZBIRD74790	M	Right	48.2	68.1	3.7	4.5	19.9	16.65	0.2444933
MVZBIRD74790	M	Left	49.7	66.3	3.6	4.5	16.6	16.2	0.2443438

Corvus corax principalis									
CAT. #	Sex	Side	Diaphysis	Length	Width	Depth	Diff.	Area	Robustness
MVZBIRD134086	F	Right	43.4	61.8	3.8	5.2	18.4	19.76	0.3197411
MVZBIRD134086	F	Left	44.3	62.3	3.8	5.1	18	19.38	0.3110754
MVZBIRD62345	-	Right	44.3	65.8	4	5.2	21.5	20.8	0.3161094
MVZBIRD62345	-	Left	44.8	66	3.8	4.9	21.2	18.62	0.2821212

APPENDIX C: KRUSKAL-WALLIS RESULTS

Table C. 1. Kruskal-Wallis Values for *Coragyps occidentalis* and *C. atratus* TMT length

K (Observed value)	30.926
K (Critical value)	9.488
DF	4
p-value (one-tailed)	< 0.0001
alpha	0.05

Table C. 2. Multiple pairwise comparison using Dunn's procedure for Black Vulture TMT length. P-values in green correlate groups, p-values in bold indicate significance. Bonferroni correction automatically calculated based on sample size.

Sample	Frequency	Sum of ranks	Mean of ranks	Groups	
0	36	5547.000	154.083	A	
21	13	1467.000	112.846	A	B
14	92	9184.000	99.826		B
18	60	5217.500	86.958		B
35	9	739.500	82.167		B

p-values:

	0	14	18	21	35
0	1	**< 0.0001**	**< 0.0001**	0.036	**0.001**
14	**< 0.0001**	1	0.202	0.470	0.405
18	**< 0.0001**	0.202	1	0.164	0.825
21	0.036	0.470	0.164	1	0.244
35	**0.001**	0.405	0.825	0.244	1

Bonferroni corrected significance level: 0.005

Table C. 3. Kruskal-Wallis analysis of Black Vulture TMT depth

K (Observed value)	17.980
K (Critical value)	9.488
DF	4
p-value (one-tailed)	0.001
alpha	0.05

Table C. 4. Multiple pairwise comparison using Dunn's procedure for Black Vulture TMT depth
P-values in green correlate groups, p-values in bold indicate significance. Bonferroni correction automatically calculated based on sample size.

Sample	Frequency	Sum of ranks	Mean of ranks	Groups	
0	36	5184.500	144.014	A	
21	13	1313.000	101.000	A	B
18	60	6047.000	100.783		B
35	9	905.500	100.611		B
14	92	8705.000	94.620		B

p-values:

	0	14	18	21	35
0	1	**< 0.0001**	**0.001**	0.028	0.055
14	**< 0.0001**	1	0.540	0.722	0.777
18	**0.001**	0.540	1	0.991	0.994
21	0.028	0.722	0.991	1	0.988
35	0.055	0.777	0.994	0.988	1

Bonferroni corrected significance level: 0.005

Table C. 5. Kruskal-Wallis analysis of Black Vulture TMT midshaft area

K (Observed value)	12.175
K (Critical value)	9.488
DF	4
p-value (one-tailed)	0.016
alpha	0.05

Table C. 6. Multiple pairwise comparison using Dunn's procedure for Black Vulture TMT midshaft area.P-values in green correlate groups, p-values in bold indicate significance. Bonferroni correction automatically calculated based on sample size.

Sample	Frequency	Sum of ranks	Mean of ranks	Groups	
0	36	4813.000	133.694	A	
35	9	1036.500	115.167	A	B
18	60	6484.000	108.067	A	B
21	13	1245.500	95.808	A	B
14	92	8576.000	93.217		B

p-values:

	0	14	18	21	35
0	1	**0.001**	0.045	0.054	0.413
14	**0.001**	1	0.141	0.886	0.301
18	0.045	0.141	1	0.510	0.744
21	0.054	0.886	0.510	1	0.463
35	0.413	0.301	0.744	0.463	1

Bonferroni corrected significance level: 0.005

Table C. 7. Kruskal-Wallis analysis of Common Raven TMT depth

K (Observed value)	38.374
K (Critical value)	14.067
DF	7
p-value (one-tailed)	< 0.0001
alpha	0.05

Table C. 8. Multiple pairwise comparison using Dunn's procedure for Common Raven TMT depth P-values in green correlate groups, p-values in bold indicate significance. Bonferroni correction automatically calculated based on sample size.

Sample	Frequency	Sum of ranks	Mean of ranks	Groups	
0	15	1988.500	132.567	A	
21	1	127.000	127.000	A	
16	6	670.500	111.750	A	
14	32	3262.000	101.938	A	
18	14	1278.000	91.286	A	B
29	9	639.000	71.000	A	B
9	81	5375.500	66.364		B
11	7	354.500	50.643		B

p-values:

	0	9	11	14	16	18	21	29
0	1	**< 0.0001**	**0.000**	0.040	0.366	0.020	0.910	0.002
9	**< 0.0001**	1	0.403	**0.000**	0.024	0.071	0.206	0.782
11	**0.000**	0.403	1	0.010	0.021	0.066	0.134	0.397
14	0.040	**0.000**	0.010	1	0.644	0.486	0.605	0.085
16	0.366	0.024	0.021	0.644	1	0.379	0.767	0.105
18	0.020	0.071	0.066	0.486	0.379	1	0.469	0.319
21	0.910	0.206	0.134	0.605	0.767	0.469	1	0.265
29	0.002	0.782	0.397	0.085	0.105	0.319	0.265	1

Bonferroni corrected significance level: 0.0018

Table C. 9. Kruskal-Wallis analysis of Common Raven midshaft area

K (Observed value)	16.986
K (Critical value)	14.067
DF	7
p-value (one-tailed)	0.017
alpha	0.05

Table C. 10. Multiple pairwise comparison using Dunn's procedure for Common Raven TMT midshaft area. P-values in green correlate groups, p-values in bold indicate significance. Bonferroni correction automatically calculated based on sample size.

Sample	Frequency	Sum of ranks	Mean of ranks	Groups	
0	15	1773.000	118.200	A	
16	6	677.500	112.917	A	B
21	1	107.000	107.000	A	B
14	32	2894.000	90.438	A	B
18	14	1138.000	81.286	A	B
9	81	6138.500	75.784		B
29	9	559.000	62.111		B
11	7	408.000	58.286		B

p-values:

	0	9	11	14	16	18	21	29
0	1	**0.002**	0.006	0.063	0.819	0.038	0.820	0.005
9	**0.002**	1	0.352	0.142	0.066	0.691	0.516	0.415
11	0.006	0.352	1	0.107	0.040	0.298	0.340	0.874
14	0.063	0.142	0.107	1	0.290	0.550	0.733	0.116
16	0.819	0.066	0.040	0.290	1	0.175	0.909	0.044
18	0.038	0.691	0.298	0.550	0.175	1	0.603	0.347
21	0.820	0.516	0.340	0.733	0.909	0.603	1	0.373
29	0.005	0.415	0.874	0.116	0.044	0.347	0.373	1

Bonferroni corrected significance level: 0.0018

Table C. 11. Kruskal-Wallis analysis of Common Raven robustness index

K (Observed value)	15.521
K (Critical value)	14.067
DF	7
p-value (one-tailed)	0.030
alpha	0.05

Table C. 12. Multiple pairwise comparison using Dunn's procedure for Common Raven TMT robustness. P-values in green correlate groups, p-values in bold indicate significance. Bonferroni correction automatically calculated based on sample size.

Sample	Frequency	Sum of ranks	Mean of ranks	Groups
0	15	1738.000	115.867	A
16	6	666.000	111.000	A
14	32	2937.000	91.781	A
18	14	1161.000	82.929	A
21	1	82.000	82.000	A
9	81	6127.000	75.642	A
29	9	586.000	65.111	A
11	7	398.000	56.857	A

p-values:

	0	9	11	14	16	18	21	29
0	1	0.003	0.007	0.107	0.833	0.064	0.492	0.012
9	0.003	1	0.318	0.106	0.080	0.598	0.895	0.530
11	0.007	0.318	1	0.080	0.042	0.238	0.623	0.732
14	0.107	0.106	0.080	1	0.366	0.563	0.840	0.139
16	0.833	0.080	0.042	0.366	1	0.229	0.574	0.068
18	0.064	0.598	0.238	0.563	0.229	1	0.985	0.383
21	0.492	0.895	0.623	0.840	0.574	0.985	1	0.737
29	0.012	0.530	0.732	0.139	0.068	0.383	0.737	1

Bonferroni corrected significance level: 0.0018

Table C. 13. Kruskal-Wallis analysis of Yellow-Billed Magpie TMT length

K (Observed value)	26.065
K (Critical value)	12.592
DF	6
p-value (one-tailed)	0.000
alpha	0.05

Table C. 14. Multiple pairwise comparison using Dunn's procedure for Yellow-Billed Magpie TMT length. P-values in green correlate groups, p-values in bold indicate significance. Bonferroni correction automatically calculated based on sample size

Sample	Frequency	Sum of ranks	Mean of ranks	Groups	
18	2	60.500	30.250	A	
16	3	84.500	28.167	A	
14	11	261.500	23.773	A	
11	2	46.500	23.250	A	B
9	2	35.000	17.500	A	B
29	1	15.000	15.000	A	B
0	13	92.000	7.077		B

p-values:

	0	9	11	14	16	18	29
0	1	0.168	0.032	< **0.0001**	**0.001**	**0.002**	0.443
9	0.168	1	0.564	0.412	0.241	0.200	0.838
11	0.032	0.564	1	0.946	0.589	0.482	0.499
14	< **0.0001**	0.412	0.946	1	0.498	0.397	0.399
16	**0.001**	0.241	0.589	0.498	1	0.819	0.252
18	**0.002**	0.200	0.482	0.397	0.819	1	0.211
29	0.443	0.838	0.499	0.399	0.252	0.211	1

Bonferroni corrected significance level: 0.0024

Table C. 15. Kruskal-Wallis analysis of Yellow-Billed Magpie TMT width

K (Observed value)	13.543
K (Critical value)	12.592
DF	6
p-value (one-tailed)	0.035
alpha	0.05

Table C. 16. Multiple pairwise comparison using Dunn's procedure for Yellow-Billed Magpie TMT width. P-values in green correlate groups, p-values in bold indicate significance. Bonferroni correction automatically calculated based on sample size

Sample	Frequency	Sum of ranks	Mean of ranks	Groups
29	1	32.500	32.500	A
16	3	86.500	28.833	A
11	2	47.000	23.500	A
14	11	222.000	20.182	A
18	2	34.000	17.000	A
9	2	30.500	15.250	A
0	13	142.500	10.962	A

p-values:

	0	9	11	14	16	18	29
0	1	0.569	0.095	0.023	0.005	0.422	0.036
9	0.569	1	0.405	0.517	0.133	0.860	0.155
11	0.095	0.405	1	0.663	0.555	0.512	0.458
14	0.023	0.517	0.663	1	0.180	0.676	0.234
16	0.005	0.133	0.555	0.180	1	0.190	0.748
18	0.422	0.860	0.512	0.676	0.190	1	0.201
29	0.036	0.155	0.458	0.234	0.748	0.201	1

Bonferroni corrected significance level: 0.0024

Table C. 17. Kruskal-Wallis analysis of Western Meadowlark TMT length

K (Observed value)	21.767
K (Critical value)	9.488
DF	4
p-value (one-tailed)	0.000
alpha	0.05

Table C. 18. Multiple pairwise comparison using Dunn's procedure for Western Meadowlark TMT length.P-values in green correlate groups, p-values in bold indicate significance. Bonferroni correction automatically calculated based on sample size

Sample	Frequency	Sum of ranks	Mean of ranks	Groups	
14	2	71.000	35.500	A	
9	15	398.000	26.533	A	
29	10	233.000	23.300	A	
18	6	123.000	20.500	A	B
0	8	36.000	4.500		B

p-values:

	0	9	14	18	29
0	1	**< 0.0001**	**0.001**	0.013	**0.001**
9	**< 0.0001**	1	0.319	0.296	0.508
14	**0.001**	0.319	1	0.124	0.188
18	0.013	0.296	0.124	1	0.650
29	**0.001**	0.508	0.188	0.650	1

Bonferroni corrected significance level: 0.005

Table C. 19. Kruskal-Wallis analysis of Western Meadowlark TMT width

K (Observed value)	22.949
K (Critical value)	9.488
DF	4
p-value (one-tailed)	0.000
alpha	0.05

Table C. 20. Multiple pairwise comparison using Dunn's procedure for Western Meadowlark TMT width.P-values in green correlate groups, p-values in bold indicate significance. Bonferroni correction automatically calculated based on sample size

Sample	Frequency	Sum of ranks	Mean of ranks	Groups	
18	6	175.500	29.250	A	
29	10	287.000	28.700	A	
14	2	53.000	26.500	A	
9	15	309.500	20.633	A	
0	8	36.000	4.500		B

p-values:

	0	9	14	18	29
0	1	**0.002**	0.019	**0.000**	< **0.0001**
9	**0.002**	1	0.512	0.133	0.096
14	0.019	0.512	1	0.777	0.811
18	**0.000**	0.133	0.777	1	0.929
29	< **0.0001**	0.096	0.811	0.929	1

Bonferroni corrected significance level: 0.005

Table C. 21. Kruskal-Wallis analysis of Western Meadowlark TMT depth

K (Observed value)	18.415
K (Critical value)	9.488
DF	4
p-value (one-tailed)	0.001
alpha	0.05

Table C. 22. Multiple pairwise comparison using Dunn's procedure for Western Meadowlark TMT depth. P-values in green correlate groups, p-values in bold indicate significance. Bonferroni correction automatically calculated based on sample size

Sample	Frequency	Sum of ranks	Mean of ranks	Groups	
29	10	276.000	27.600	A	
9	15	363.500	24.233	A	
14	2	47.000	23.500	A	B
18	6	133.000	22.167	A	B
0	8	41.500	5.188		B

p-values:

	0	9	14	18	29
0	1	**0.000**	0.052	0.008	**< 0.0001**
9	**0.000**	1	0.935	0.719	0.489
14	0.052	0.935	1	0.891	0.657
18	0.008	0.719	0.891	1	0.377
29	**< 0.0001**	0.489	0.657	0.377	1

Bonferroni corrected significance level: 0.005

Table C. 23. Kruskal-Wallis analysis of Western Meadowlark TMT midshaft area

K (Observed value)	20.848
K (Critical value)	9.488
DF	4
p-value (one-tailed)	0.000
alpha	0.05

Table C. 24. Multiple pairwise comparison using Dunn's procedure for Western Meadowlark TMT midshaft area. P-values in green correlate groups, p-values in bold indicate significance. Bonferroni correction automatically calculated based on sample size

Sample	Frequency	Sum of ranks	Mean of ranks	Groups	
29	10	291.000	29.100	A	
18	6	152.000	25.333	A	
14	2	47.500	23.750	A	
9	15	334.500	22.300	A	
0	8	36.000	4.500		B

p-values:

	0	9	14	18	29
0	1	**0.001**	0.042	**0.001**	**< 0.0001**
9	**0.001**	1	0.872	0.600	0.164
14	0.042	0.872	1	0.871	0.564
18	**0.001**	0.600	0.871	1	0.542
29	**< 0.0001**	0.164	0.564	0.542	1

Bonferroni corrected significance level: 0.005

Table C. 25. Kruskal-Wallis analysis of Western Meadowlark TMT robustness

K (Observed value)	21.128
K (Critical value)	9.488
DF	4
p-value (one-tailed)	0.000
alpha	0.05

Table C. 26. Multiple pairwise comparison using Dunn's procedure for Western Meadowlark TMT robustness. P-values in green correlate groups, p-values in bold indicate significance. Bonferroni correction automatically calculated based on sample size

Sample	Frequency	Sum of ranks	Mean of ranks	Groups	
29	10	290.000	29.000	A	
18	6	163.500	27.250	A	
9	15	328.500	21.900	A	
14	2	42.000	21.000	A	B
0	8	37.000	4.625		B

p-values:

	0	9	14	18	29
0	1	**0.001**	0.084	**0.000**	**< 0.0001**
9	**0.001**	1	0.920	0.355	0.147
14	0.084	0.920	1	0.523	0.389
18	**0.000**	0.355	0.523	1	0.777
29	**< 0.0001**	0.147	0.389	0.777	1

Bonferroni corrected significance level: 0.005